Article

Cell Metabolism

LRP5 Regulates Human Body Fat Distribution by Modulating Adipose Progenitor Biology in a Dose- and Depot-Specific Fashion

Graphical Abstract

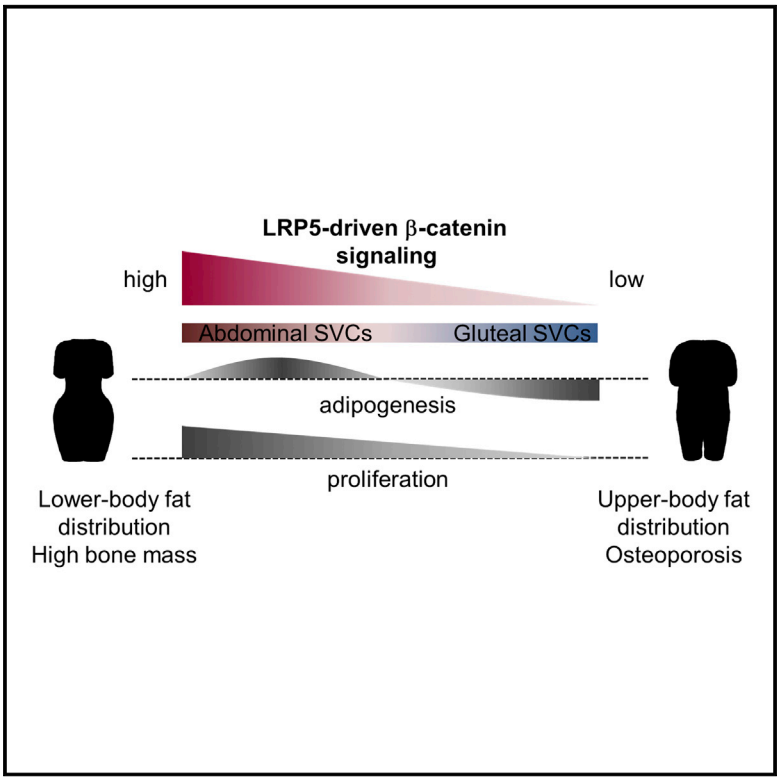

Authors

Nellie Y. Loh, Matt J. Neville, ..., Fredrik Karpe, Constantinos Christodoulides

Correspondence

fredrik.karpe@ocdem.ox.ac.uk (F.K.), costas.christodoulides@ocdem.ox.ac.uk (C.C.)

In Brief

Loh et al. identify the WNT co-receptor LRP5 as a regulator of human body fat distribution, an independent predictor of diabetes and cardiovascular disease risk. Studying *LRP5* gene variant carriers and human fat progenitors, they show that LRP5 differentially modulates regional adipose progenitor biology by titrating WNT/β-catenin signaling dosage.

Highlights

- Carriers of *LRP5* variants display altered body fat distribution
- *LRP5* is more highly expressed in abdominal versus gluteal fat progenitor cells
- *LRP5* knockdown in both progenitor types leads to different biological responses
- LRP5 modulates fat progenitor biology by controlling β-catenin signaling dosage

Loh et al., 2015, Cell Metabolism *21*, 262–272
February 3, 2015
http://dx.doi.org/10.1016/j.cmet.2015.01.009

CellPress

Cell Metabolism
Article

LRP5 Regulates Human Body Fat Distribution by Modulating Adipose Progenitor Biology in a Dose- and Depot-Specific Fashion

Nellie Y. Loh,[1] Matt J. Neville,[1,2] Kyriakoula Marinou,[1,3] Sarah A. Hardcastle,[4] Barbara A. Fielding,[1,5] Emma L. Duncan,[6,7] Mark I. McCarthy,[1,2] Jonathan H. Tobias,[4] Celia L. Gregson,[4] Fredrik Karpe,[1,2,*] and Constantinos Christodoulides[1,*]

[1]Oxford Centre for Diabetes, Endocrinology and Metabolism, Radcliffe Department of Medicine, University of Oxford, Oxford OX3 7LE, UK
[2]NIHR Oxford Biomedical Research Centre, Oxford University Hospitals NHS Trust, Oxford OX3 7LE, UK
[3]Department of Experimental Physiology, Athens University School of Medicine, Athens 11527, Greece
[4]Musculoskeletal Research Unit, School of Clinical Sciences, University of Bristol, Bristol BS10 5NB, UK
[5]Department of Nutritional Sciences, Faculty of Health and Medical Sciences, University of Surrey, Guildford GU2 7XH, UK
[6]University of Queensland Diamantina Institute, School of Medicine and University of Queensland Centre for Clinical Research, Faculty of Medicine and Biomedical Sciences, University of Queensland, Woolloongabba, QLD 4102, Australia
[7]Department of Endocrinology, Royal Brisbane and Women's Hospital, Butterfield Street, Herston, QLD 4029, Australia
*Correspondence: fredrik.karpe@ocdem.ox.ac.uk (F.K.), costas.christodoulides@ocdem.ox.ac.uk (C.C.)
http://dx.doi.org/10.1016/j.cmet.2015.01.009

SUMMARY

Common variants in WNT pathway genes have been associated with bone mass and fat distribution, the latter predicting diabetes and cardiovascular disease risk. Rare mutations in the WNT co-receptors *LRP5* and *LRP6* are similarly associated with bone and cardiometabolic disorders. We investigated the role of LRP5 in human adipose tissue. Subjects with gain-of-function *LRP5* mutations and high bone mass had enhanced lower-body fat accumulation. Reciprocally, a low bone mineral density-associated common *LRP5* allele correlated with increased abdominal adiposity. Ex vivo *LRP5* expression was higher in abdominal versus gluteal adipocyte progenitors. Equivalent knockdown of *LRP5* in both progenitor types dose-dependently impaired β-catenin signaling and led to distinct biological outcomes: diminished gluteal and enhanced abdominal adipogenesis. These data highlight how depot differences in WNT/β-catenin pathway activity modulate human fat distribution via effects on adipocyte progenitor biology. They also identify LRP5 as a potential pharmacologic target for the treatment of cardiometabolic disorders.

INTRODUCTION

Obesity is associated with the development of insulin resistance, linked to the pathogenesis of type 2 diabetes (T2D) and cardiovascular disease (CVD). Nonetheless, adverse metabolic sequelae are not uniformly observed in obese individuals. While subjects with abdominal obesity display an increased prevalence of CVD, similarly overweight individuals with gluteofemoral fat distribution are protected from cardiometabolic disorders (Yusuf et al., 2005). Consistent with epidemiologic findings, physiological studies have shown that the gluteofemoral white adipose tissue (WAT) depot displays differential fatty acid (FA) handling compared to the subcutaneous (SC) abdominal WAT depot (Jensen, 2008; Karpe and Pinnick, 2014). By favoring the long-term storage of FAs, gluteofemoral fat may protect skeletal muscle from ectopic lipid accumulation and lipotoxicity, which triggers insulin resistance (Schenk et al., 2008). Gluteofemoral fat may also contribute to improved metabolic risk by secreting a more beneficial adipocytokine profile than SC abdominal and visceral fat (Fontana et al., 2007; Turer et al., 2011). Adipose-derived hormones and cytokines directly modulate systemic insulin sensitivity (Qatanani and Lazar, 2007).

WAT expands by an increase in adipocyte number (hyperplasia) and size (hypertrophy) (Spalding et al., 2008; Tchoukalova et al., 2010). Adipocytes derive from mesenchymal stem cells (MSCs) and preadipocytes that reside in the stromovascular fraction of WAT. Several clinical and experimental studies indicate that discrete fat depots arise from distinct precursors with inherently different proliferative and adipogenic properties (Billon and Dani, 2012; Semple et al., 2011; Tchkonia et al., 2006). It is further postulated that developmental pathways play a key role in establishing the distinct identities of adipose progenitors from separate locations and thus in determining (1) the relative size of fat depots, by determining adipocyte number (and size) within each depot, and (2) the function of WAT depots, by modulating expression of adipogenic genes and their downstream targets. Consistent with this hypothesis, stromovascular cells (SVCs) isolated from discrete fat depots exhibit distinct developmental gene expression profiles (Gesta et al., 2006; Tchkonia et al., 2007). Furthermore, in a genome-wide association study (GWAS) meta-analysis, 4 of the 13 identified loci associated with body mass index (BMI)-adjusted waist-to-hip ratio (WHR), a measure of body fat distribution, mapped in or near developmental genes (Heid et al., 2010). Notably two of these, *RSPO3* and *ZNRF3*, constitute WNT signaling modulators. A locus near *RSPO3*, distinct from the WHR-associated signal, was also shown

Table 1. Anthropometry, Plasma Biochemistry, and DXA-Derived Measures of Body Fat Distribution of HBM Patients with *LRP5* Gain-of-Function Mutations from Three Kindreds versus Those of Their Age-, Gender-, and BMI-Matched OBB Controls

	S1	Controls for S1	S2	Controls for S2	S3	Controls for S3	S4	Controls for S4	S5	Controls for S5	S6	Controls for S6
n	–	129 (77[a])	–	74 (42[a])	–	105 (65[a])	–	51 (33[a])	–	55 (33[a])	–	102 (59[a])
Age (years)	45	44.8 (44.3–45.2)	68[c]	49.1 (48.9–49.3)	50[c]	48.0 (47.7–48.4)	28[c]	31.9 (31.5–32.2)	38	38.1 (36.9–39.3)	34[c]	34.6 (34.1–35.1)
Gender	F	F	F	F	F	F	M	M	F	F	M	M
BMI (kg/m^2)	27.2	27.2 (27.1–27.3)	27.3	27.2 (27.0–27.3)	26.0	26.0 (25.9–26.0)	21.8	22.0 (21.8–22.1)	35.1	35.0 (34.8–35.2)	28.8[c]	28.4 (28.2–28.5)
HOMA-IR	0.6[c]	1.7 (1.6–1.8)	1.7	1.7 (1.6–1.9)	1.6[b,c]	1.7 (1.6–1.8)	0.6[c]	1.5 (1.3–1.6)	1.2[c]	2.4 (2.1–2.7)	1.3[c]	2.1 (2.0–2.3)
Tissue legs, % fat	43.5[c]	40.0 (38.9–41.1)	44.2[c]	39.6 (38.1–41.0)	48.4[c]	39.8 (38.7–40.8)	19.7	20.5 (18.9–22.1)	50.2[c]	45.0 (43.1–46.8)	31.1[c]	26.4 (25.1–27.6)
Tissue android, % fat	35.6[c]	41.5 (40.0–42.9)	43.7	42.4 (40.2–44.7)	43.9[c]	41.1 (39.4–42.8)	11.6[c]	21.0 (18.5–23.5)	55.3	53.9 (52.3–55.5)	35.5[c]	39.6 (38.3–40.9)
Android:leg fat ratio (%)	16.4[c]	22.6 (21.1–24.1)	21.5[c]	24.7 (22.0–27.3)	18.9[c]	23.2 (21.4–25.0)	11.0[c]	22.0 (19.7–24.4)	21.5[c]	29.2 (26.3–32.1)	24.8[c]	35.9 (33.8–37.9)
Android:total fat ratio (%)	6.7[c]	7.8 (7.6–8.1)	7.5[c]	8.2 (7.7–8.6)	7.0[c]	7.9 (7.6–8.2)	4.3[c]	7.1 (6.6–7.5)	8.6[c]	9.3 (8.9–9.8)	8.6[c]	9.8 (9.6–10.1)
Central:peripheral fat mass ratio (g/g)	12.9[c]	17.0 (16.0–18.0)	16.3[c]	18.4 (16.6–20.1)	14.1[c]	17.4 (16.2–18.6)	8.7[c]	16.9 (15.2–18.6)	18.6[c]	21.7 (19.8–23.6)	19.1[c]	26.3 (25.0–27.6)

Data for controls are means (95% CI). n, number of age-, gender-, and BMI-matched controls. Subjects from Kindred 1 (S1, S2) and Kindred 2 (S3, S4) carry the A242T mutation; those from Kindred 3 (S5, S6) carry the N198S mutation. NB: We were unable to match subjects S2 and S4 for age. HBM, high bone mass; CI, confidence interval; BMI, body mass index; HOMA-IR, homeostasis model assessment-estimated insulin resistance. See also Table S2 and Figure S1.

[a]Number of controls with DXA measurements.

[b]Actual value is below the 95% CI.

[c]Values below/above the 95% CI.

to be associated with bone mineral density (BMD) at genome-wide significance (Duncan et al., 2011; Estrada et al., 2012).

WNTs are a family of 19 secreted glycoproteins acting locally via multiple pathways to regulate adult tissue homeostasis (Clevers and Nusse, 2012). In the β-catenin ("canonical") cascade, WNT binding to Frizzled (FZD) receptors and low-density lipoprotein receptor-related protein (LRP) 5/6 co-receptors leads to nuclear accumulation of the transcriptional co-activator β-catenin, which, paired with LEF/TCF transcription factors, dose-dependently modulates (generally activates) WNT target gene expression. WNTs also signal through "non-canonical" pathways. In the planar cell polarity (PCP) pathway, WNT binding to FZD activates JNK and stimulates AP1-dependent transcription. In the WNT/Ca^{2+} pathway, WNT/FZD interaction triggers intracellular Ca^{2+} release and calmodulin-dependent protein kinase-2A (CAMK2A) activation. Canonical and non-canonical pathways are thought to be mutually antagonistic (Grumolato et al., 2010; Weidinger and Moon, 2003).

WNT signaling is a key regulator of MSC biology (Christodoulides et al., 2009; Krishnan et al., 2006). Canonical signaling, the best-studied pathway, which critically relies on LRP5 and LRP6 co-receptors for activation, has been shown to repress adipogenesis and stimulate osteoblastogenesis. Accordingly, patients carrying rare gain-of-function (GoF) *LRP5* mutations exhibit high bone mass (HBM) (Boyden et al., 2002; Little et al., 2002). Reciprocally, rare loss-of-function (LoF) *LRP5* mutations lead to osteoporosis (Ai et al., 2005; Gong et al., 2001), which, in a study of 12 affected probands from two families, was coupled with an increased prevalence of T2D (Saarinen et al., 2010). Finally, rare inactivating missense mutations in *LRP6* result in autosomal dominant CVD, features of the metabolic syndrome, and osteoporosis (Mani et al., 2007; Singh et al., 2013). Prompted by these and the aforementioned GWAS findings (Heid et al., 2010), we sought to determine the role of LRP5 in human WAT biology and fat distribution. Our interest in LRP5 was also stimulated by preliminary analyses showing that it was differentially expressed between SC abdominal and gluteal SVCs. Furthermore, WAT *LRP5* mRNA levels correlated with measures of regional adiposity and systemic insulin sensitivity. Herein we demonstrate that LRP5-driven β-catenin signaling regulates adipose progenitor proliferation and differentiation in a dose- and depot-specific manner, thereby modulating human body fat distribution.

RESULTS

HBM-Causing *LRP5* Mutations Are Associated with Lower-Body Fat Accumulation

We examined the adipose and metabolic phenotype of three pedigrees with extreme HBM secondary to rare heterozygous GoF *LRP5* mutations. Compared to age-, gender-, and BMI-matched Oxford Biobank (OBB) controls, HBM *LRP5* mutation carriers had an increased amount of lower-body fat as determined by whole-body dual energy X-ray absorptiometry (DXA). In particular, all overweight/obese (BMI $\geq$ 25) HBM subjects with *LRP5* mutations (n = 5 of 6 individuals in total; S1–S3, S5, S6) had a higher tissue percent fat specifically in their legs (Table 1). Furthermore, all affected individuals displayed lower android/leg, android/total, and central/peripheral fat mass ratios

Table 2. Comparison of Anthropometry and DXA-Derived Measures of Body Fat Distribution of HBM Subjects With and Without *LRP5* Gain-of-Function Mutations, Matched for Age, Gender, and BMI

	LRP5 HBM (n = 6)	Non-*LRP5* HBM (n = 18)
	Mean ± SD	Mean (95% CI)
Age (years)	43.0 ± 14.5	41.9 (31.0, 52.7)
BMI (kg/m^2)	27.7 ± 4.3	27.7 (25.5, 29.9)
Tissue legs, % fat	39.5 ± 11.8	36.3 (30.3, 42.2)
Tissue android, % fat	37.6 ± 14.7	46.8 (40.3, 53.3)[a]
Android:leg fat ratio (%)	19.0 ± 4.8	29.5 (26.5, 32.4)[b]
Android:total fat ratio (%)	7.1 ± 1.6	9.1 (8.4, 9.7)[b]
Central:peripheral fat mass ratio (g/g)	15.0 ± 3.9	22.0 (19.9, 24.1)[b]

LRP5 HBM subjects (Tables 1 and S2) were matched with non-*LRP5* HBM subjects on age (within 6 years), sex, and BMI (kg/m^2), based on radius matching with a ratio 3:1, using a multi-level regression model clustering by match set. HBM, high bone mass; BMI, body mass index; CI, confidence interval. See also Table S1.
[a]$p < 0.05$.
[b]$p \leq 0.001$.

Table 3. Association Studies of the BMD-Associated *LRP5* SNP Rs599083 and DXA-Derived Measures of Body Fat Distribution of Subjects from the Oxford Biobank

	Rs599083					
	Adjusted for age, gender, and BMI			Adjusted for age, gender, BMI, and BMD		
Trait	p value	β	n	p value	β	n
Tissue leg, % fat	0.4	0.007	3,289	1	0.002	3,289
Tissue android, % fat	0.004[a]	0.033	3,289	0.02[a]	0.027	3,289
Android:leg fat ratio (%)	0.008[a]	0.028	3,289	0.02[a]	0.025	3,289
Android:total fat ratio (%)	0.006[a]	0.031	3,289	0.01[a]	0.027	3,289
Central:peripheral ratio (g/g)	0.007 [a]	0.028	3,289	0.02[a]	0.024	3,289
BMD (g/cm^2)	9×10^{-5}[a]	−0.058	3,289	–	–	–

Effect allele: guanine nucleotide. Effect allele frequency: 0.34. BMD, bone mineral density; p value, empirical p value; β, standardized beta value; n, number of subjects. Data are from 1,438 men and 1,851 women. See also Tables S3–S5 and Figure S2.
[a]Significant p values.

(Table 1). This adipose phenotype was not driven by the HBM, as HBM *LRP5* mutation carriers had a decreased upper-to-lower-body fat ratio even when compared with matched non-*LRP5* HBM cases (n = 18) (Table 2). Similar results were obtained when comparing age-, gender-, and BMI-adjusted DXA data from *LRP5* HBM cases versus the rest of the (non-*LRP5*) HBM cohort (n = 134) (Table S1). *LRP5* HBM individuals also exhibited enhanced insulin sensitivity as determined by lower HOMA-IR and fasting insulin levels relative to OBB controls (Tables 1 and S2). One exception was subject S2 (68 years old), whom we were able to compare only with 49–50 year old gender- and BMI-matched controls. Finally, ex vivo gene expression analyses of fractionated SC adipose cells revealed lower inflammatory gene transcript levels in *LRP5* HBM individuals (n = 4; subjects S1, S4–S6) versus OBB controls (n = 24–25) (Figure S1A). We conclude that rare, GoF *LRP5* mutations are associated with enhanced lower-body fat accumulation, a favorable metabolic profile, and reduced WAT inflammation.

A Low BMD-Associated Allele in *LRP5* Correlates with Upper-Body Fat Accumulation

To further investigate the role of LRP5 in regulating regional adiposity, we explored the association between a common *LRP5* single nucleotide polymorphism (SNP) and DXA-derived measures of fat distribution in 3,289 OBB volunteers. Rs599083 is an intronic SNP shown to be significantly associated with lumbar spine BMD in a GWAS meta-analysis (Rivadeneira et al., 2009). Of note, rs599083 showed modest evidence of association with fat distribution within the OBB cohort (Table 3). Specifically, the low BMD-associated minor allele at this locus correlated with increased age-, gender-, and BMI-adjusted android tissue percent fat and android/total and central/peripheral fat mass ratios. These associations were attenuated following adjustment for BMD, in keeping with rs599083 being an overlapping signal for bone and fat traits (Table 3). Based on the established association between LoF *LRP5* mutations and osteoporosis (Ai et al., 2005; Gong et al., 2001), we presume that this allele is associated with reduced LRP5 function, which, according to gene expression analyses from 37 OBB subjects (Figure S2A) and eQTL data from the MuTHER consortium (http://www.muther.ac.uk), is not driven by changes in adipose *LRP5* mRNA levels. We also undertook histological analyses of SC abdominal WAT from 18 overweight and obese individuals. Subject characteristics are shown in Table S3. These revealed that adipocyte numbers in android fat tended to be lower in carriers of the low BMD-associated allele at rs599083 (GG, GT) versus homozygous carriers of the common allele (TT) ($p = 0.05$). This effect was primarily due to a reduction in small adipocytes (Figures S2B and S2C). No associations between rs599083 and anthropometric measures of fat distribution were identified within the OBB (Table S4). Nonetheless, and consistent with our findings, this SNP was weakly associated with BMI-adjusted waist circumference (WC) in females ($p = 0.001$ for association, $\beta = 0.016$ for the minor allele) in the publicly available sex-stratified GIANT data set (Randall et al., 2013). It should be noted that associations between waist and hip circumferences and the respective regional fat masses (android and gynoid) within the OBB had rho values of ~0.5 (Table S5). We conclude that, mirroring the effects of rare GoF *LRP5* mutations, a common *LRP5* allele that is presumably associated with reduced LRP5 function correlates with modestly increased upper-body fat accumulation.

LRP5 Is More Highly Expressed in Abdominal Than Gluteal Adipose Progenitors

In order to gain mechanistic insights into the effects of LRP5 on fat distribution, we examined the *LRP5* gene expression pattern

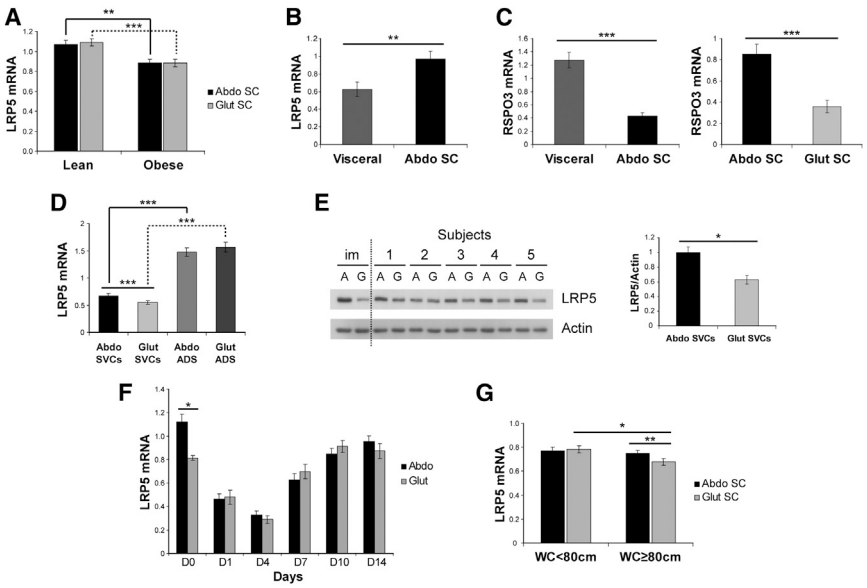

Figure 1. *LRP5* Expression in Human SC Abdominal, Gluteal, and Visceral WAT

(A and B) *LRP5* mRNA levels in (A) paired SC abdominal (Abdo) and gluteal (Glut) fat biopsies from lean and obese subjects (n = 20/group) and (B) paired SC abdominal and visceral fat biopsies from 16 individuals undergoing surgery. n = 7 women (age 43.6 ± 15.1 years [range 21.2–61]; BMI 30.0 ± 9.1 kg/m^2 [range 19.1–42]) and 9 men (age 63.9 ± 9.3 years [range 48–76]; BMI 26.5 ± 5 kg/m^2 [range 18.9–33.7]). Age and BMI are means ± SD.

(C) *RSPO3* mRNA levels in paired visceral versus SC abdominal fat (n = 16) and SC abdominal versus gluteal fat (n = 20).

(D) *LRP5* mRNA levels in cultured SVCs (n = 25) and mature adipocytes (ADS) (n = 24).

(E) Western blot and protein densitometry of LRP5 in immortalized (im) and primary (n = 5 pairs) SVCs from healthy subjects. A, abdominal; G, gluteal.

(F) *LRP5* mRNA levels in differentiating primary abdominal and gluteal SVCs (n = 5 pairs).

(G) Comparisons of *LRP5* mRNA levels in paired SC abdominal and gluteal WAT from women with gynoid (WC < 80 cm, n = 23) versus android (WC ≥ 80 cm, n = 24) fat distribution.

qRT-PCR data were normalized to *PGK1* and *PPIA* (A–C and G) and to *18S* (D and F). *p < 0.05, **p < 0.01, ***p < 0.001, corrected for multiple testing. Histogram data are means ± SEM. See also Tables S6, S7, and S8.

in paired SC abdominal and gluteal fat from 20 lean and 20 obese OBB volunteers (Table S6). *LRP5* expression was identical in the two depots, albeit lower in obese versus lean subjects (Figure 1A). We also compared *LRP5* gene expression in paired SC abdominal and visceral fat from 16 subjects undergoing surgery. *LRP5* mRNA levels were higher in SC abdominal WAT, in contrast to *RSPO3* gene expression, which was higher in visceral versus SC fat (Figures 1B and 1C). We next determined the expression of *LRP5* in fractionated SC abdominal and gluteal WAT (Figure 1D). *LRP5* gene expression was higher in mature adipocytes compared with SVCs from both depots. No difference in *LRP5* transcript levels was observed between abdominal and gluteal adipocytes. In contrast, *LRP5* expression was significantly higher in abdominal versus gluteal SVCs ($p = 4 \times 10^{-6}$, with Bonferroni correction). We corroborated this finding by demonstrating higher abdominal LRP5 protein level in five independent pairs of primary and one pair of immortalized (see below) SVCs (Figure 1E). Finally, we examined the *LRP5* gene expression profile in differentiating SVCs from a further five subjects. *LRP5* mRNA levels were higher in undifferentiated abdominal versus gluteal SVCs but, following induction of adipogenesis, became indistinguishable between abdominal and gluteal adipocytes (Figure 1F). In summary, *LRP5* is more highly expressed in SC versus visceral fat. Furthermore, when comparing SC depots, *LRP5* mRNA and protein levels are specifically higher in abdominal compared with gluteal adipose progenitors.

To determine whether different patterns of fat distribution (upper versus lower) are associated with differences in WAT *LRP5* gene expression, we analyzed *LRP5* mRNA levels in paired SC abdominal and gluteal fat from 47 females recruited based on WC (Table S7). A WC ≥ 80 cm is a measure of central obesity, with increased CVD risk in Europid women as defined by the International Diabetes Federation (Alberti et al., 2005). *LRP5* gene expression was selectively lower in the gluteal depot of women with android obesity (WC ≥ 80 cm) (Figure 1G). Furthermore, in partial correlation analyses, gluteal (but not abdominal) *LRP5* expression correlated negatively with upper-body fat accumulation, systemic insulin resistance, and markers of inflammation after adjustment for age, BMI, and menopausal status (Table S8). We conclude that reduced gluteal WAT *LRP5* gene expression correlates with upper-body fat accumulation and an adverse metabolic and inflammatory profile.

LRP5 Knockdown Has Distinct Biological Effects in Abdominal and Gluteal Progenitors

In light of our earlier findings, we investigated the role of LRP5 in depot-specific adipose progenitor biology using an immortalized pair of SC abdominal and gluteal SVCs. While displaying enhanced proliferation and adipogenesis (our unpublished data), these cells retain their depot-specific gene expression signatures (Pinnick et al., 2014). Stable *LRP5* knockdown (KD) in these immortalized SVCs was achieved by lentiviral transduction with two independent shRNAs (Figures 2A and S3A). Both shRNAs targeted the two protein-coding *LRP5* transcripts (http://www.ensembl.org) and were specific to *LRP5* as no change in *LRP6* mRNA levels was detected. The aim of these experiments was to compare the biological effects of equivalent *LRP5* gene dosage reduction in abdominal and gluteal SVCs rather than to completely silence *LRP5*. Clone TRCN0000033400 (sh400) gave the more efficient KD. As intended, the KD magnitude was equivalent in abdominal and gluteal progenitors (see *LRP5* gene expression panel in Figure 2A). Nonetheless, due to the higher *LRP5* gene expression in abdominal SVCs, the percentage KD achieved was 33% in abdominal versus 73% in gluteal cells compared to scrambled shRNA-transduced SVCs. Less efficient *LRP5* gene silencing (24% in abdominal versus 56% in gluteal SVCs) was achieved with shRNA clone TRCN0000033401 (sh401); again, in absolute

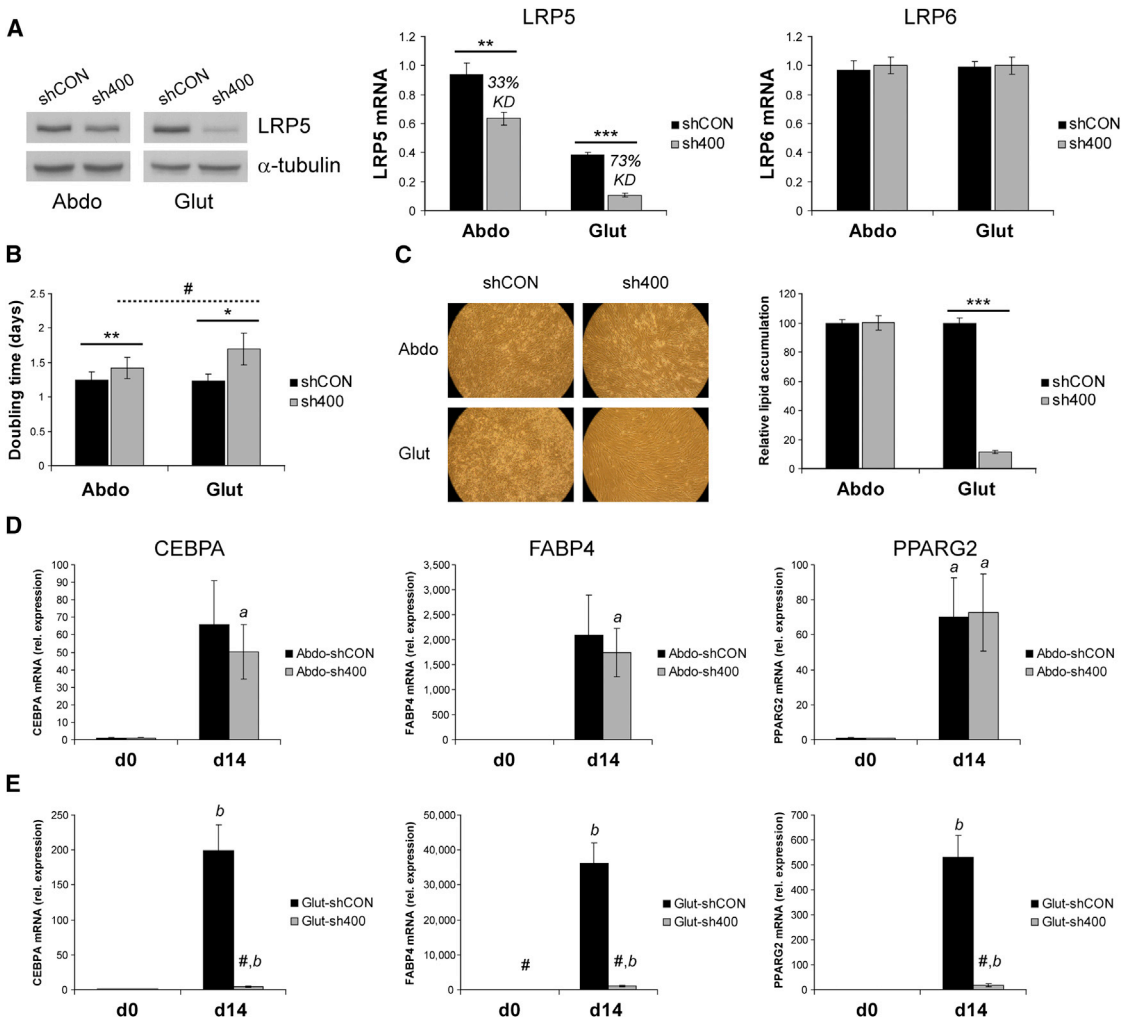

Figure 2. *LRP5* KD in Immortalized Abdominal and Gluteal SVCs Alters Cell Proliferation and Adipogenesis

(A) *LRP5* KD was confirmed by qRT-PCR and western blot analyses. *LRP6* mRNA expression was not altered by *LRP5* KD. shCON, control; sh400, *LRP5*-KD cells. $^{**}p < 0.01$, $^{***}p < 0.001$. α-tubulin was used as a western blot loading control.

(B) Doubling time of shCON and sh400 abdominal and gluteal SVCs. $^{*}p < 0.05$, $^{**}p < 0.01$, shCON versus sh400; $^{\#}p < 0.05$, Abdo-sh400 versus Glut-sh400.

(C) Representative micrographs of shCON and sh400 abdominal and gluteal SVCs at day 14 of adipogenic differentiation and histogram showing relative lipid accumulation, assessed by AdipoRed staining (n = 42 wells/group). $^{***}p < 0.001$.

(D and E) Relative mRNA levels of adipogenic genes *CEBPA*, *FABP4*, and *PPARG2* in (D) abdominal and (E) gluteal cells at baseline (d0) and day 14 (d14) of adipogenic differentiation. shCON versus sh400 cells: $^{\#}p < 0.01$; d0 versus d14 cells: $^{a}p < 0.05$, $^{b}p < 0.01$. Histogram data are means ± SEM. qRT-PCR data were normalized to *18S*. n = 5–7 independent experiments. See also Figures S1, S3, and S4.

terms *LRP5* KD was near-identical in abdominal and gluteal cells (Figure S3A). *LRP5* KD using either shRNA was associated with impaired proliferation in both abdominal and gluteal SVCs (Figure 2B and our unpublished data), a finding confirmed by *LRP5* KD in primary SVCs derived from a female subject (Figure S4A). Decreased *LRP5* expression in gluteal cells was also associated with a marked and dose-dependent inhibition of differentiation as ascertained by lipid accumulation and adipogenic gene expression (Figures 2C, 2E, S3B, and S3D). *LRP5*-KD gluteal adipocytes further exhibited heightened inflammation as determined by increased *IL6* and *MCP1* transcript levels (Figures S1B and S1C). In contrast, *LRP5* KD in abdominal progenitors using sh400 was not associated with changes in adipogenesis or adipocyte inflammation (Figures 2C, 2D, and S1B); more strikingly, stable expression of sh401 in abdominal SVCs led to enhanced differentiation (Figures S3B and S3C). Similar effects on adipogenesis were observed following sh400-mediated *LRP5* KD in female primary adipose SVCs (Figure S4B). In summary, equivalent absolute KD of *LRP5* in abdominal and gluteal progenitors leads to distinct biological outcomes that may be driven by the differential *LRP5* gene expression between the two progenitor populations.

LRP5 KD Dose-Dependently Impairs Canonical WNT Signaling in Adipose Progenitors

We examined which WNT pathway(s) were responsible for the biological actions of LRP5. *LRP5* KD in both abdominal and gluteal cells led to impaired canonical WNT signaling, as

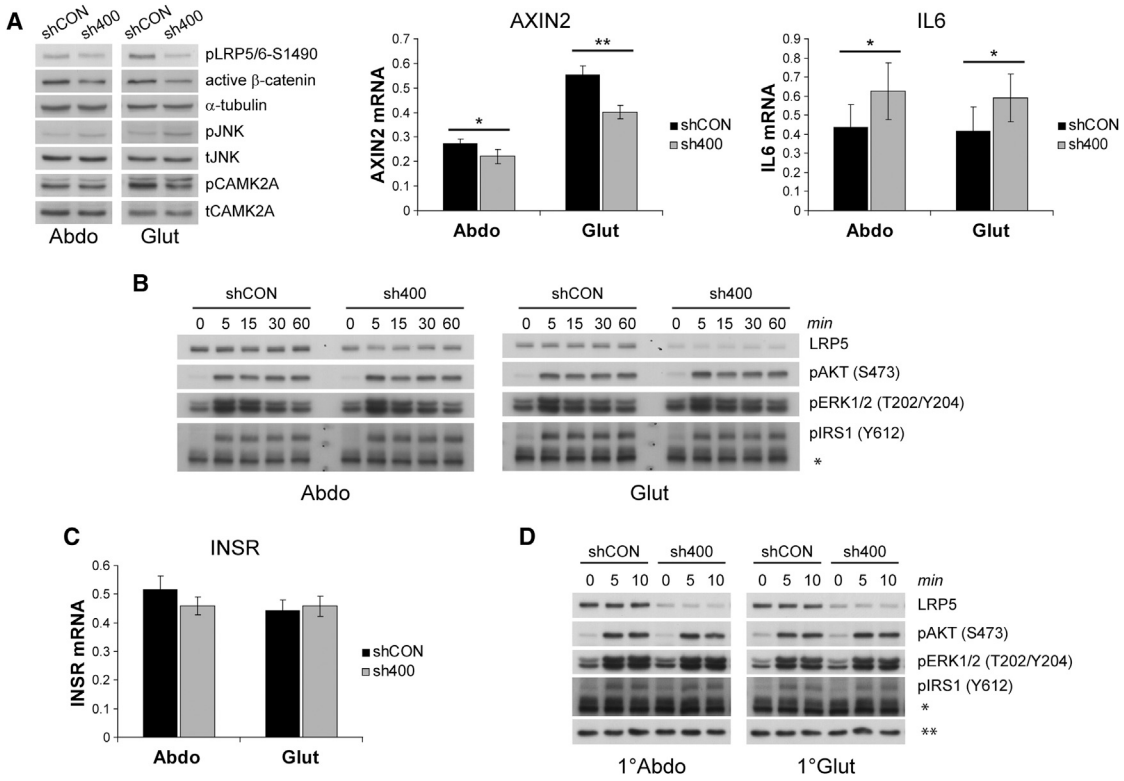

Figure 3. Effect of *LRP5* KD on Canonical and Non-Canonical WNT and Insulin Signaling Pathways in Abdominal and Gluteal SVCs

(A) Western blots for pLRP5/6-Ser1490, active β-catenin, pJNK, and pCAMK2A and qRT-PCR analyses of *AXIN2* and *IL6*, in control (shCON) and *LRP5*-KD (sh400) abdominal and gluteal immortalized SVCs. α-tubulin, total-JNK (tJNK), and total CAMK2A (tCAMK2A) were western blot loading controls. *$p < 0.05$, **$p < 0.01$.

(B) Representative western blots of shCON and sh400 abdominal and gluteal immortalized SVCs stimulated with 100 nM insulin for indicated duration. *non-specific band, used as loading control.

(C) *INSR* mRNA levels in shCON and sh400 abdominal and gluteal immortalized SVCs.

(D) Representative western blots of shCON and sh400 abdominal and gluteal primary (1°) SVCs stimulated with 10 nM insulin for indicated duration. *non-specific band detected with anti-pIRS1 (Y612) rabbit pAb, **non-specific band detected with anti-LRP5 rabbit mAb, used as loading controls. Histogram data are means ± SEM. n = 5–7 independent experiments. qRT-PCR data were normalized to *18S*. See also Figure S3.

determined by decreased active β-catenin and phosphorylated (active) LRP5/6 protein levels and reduced expression of *AXIN2*, a universal β-catenin target gene (Figures 3A and S3E). Given that β-catenin is generally thought to restrain adipogenesis, these findings are prima facie counterintuitive to the block in differentiation seen in gluteal SVCs. We next examined whether non-canonical WNT pathways were differentially regulated following *LRP5* KD in abdominal and gluteal progenitors. However, both PCP and WNT/Ca^{2+} signaling were modulated in a directionally uniform manner in *LRP5*-KD cells. Specifically, *LRP5* KD using sh400 (i.e., the more efficient shRNA) led to increased JNK phosphorylation and elevated *IL6* expression in both abdominal and gluteal SVCs, consistent with PCP pathway activation (Figure 3A). Conversely, the phosphorylated to total CAMK2A ratio was uniformly decreased in abdominal and gluteal *LRP5*-KD cells (Figures 3A, S3E, and S3F). LRP5 was shown to promote insulin signaling and adipogenesis in 3T3-L1 preadipocytes (Palsgaard et al., 2012). Hence, we asked whether insulin/IGF1 signaling was driving the actions of LRP5 on adipose progenitor biology. As shown in Figures 3B and S3G, however, neither basal nor stimulated phosphorylation of IRS1, AKT, or ERK1/2 following treatment with 100 nM insulin (i.e., the same dose used to induce adipogenesis) were altered with *LRP5* KD. Consistent with these data, no baseline change in insulin receptor (*INSR*) gene expression was detected in response to *LRP5* KD in either abdominal or gluteal SVCs (Figures 3C and S3H). We confirmed and extended these findings in *LRP5*-KD primary SVCs treated with a more physiological insulin dose (10 nM) (Figure 3D).

β-catenin has been shown to dose-dependently modulate target gene expression and stem/progenitor cell cycling and fate-determination (Hirata et al., 2013; Kielman et al., 2002; Luis et al., 2011). Given the graded effects of *LRP5* KD on abdominal and gluteal SVC proliferation and differentiation, we examined whether active β-catenin levels and β-catenin target genes were regulated in a dose-like fashion. This was indeed the case (Figures 4A and 4B). Mirroring these findings, selectively attenuating β-catenin transcriptional activity with use of the small-molecule inhibitor iCRT14 (Gonsalves et al., 2011) dose-dependently impaired adipogenesis in immortalized gluteal SVCs (Figure 4C). In contrast, low-dose iCTR14 (1 μM) enhanced adipogenesis in abdominal progenitors while higher

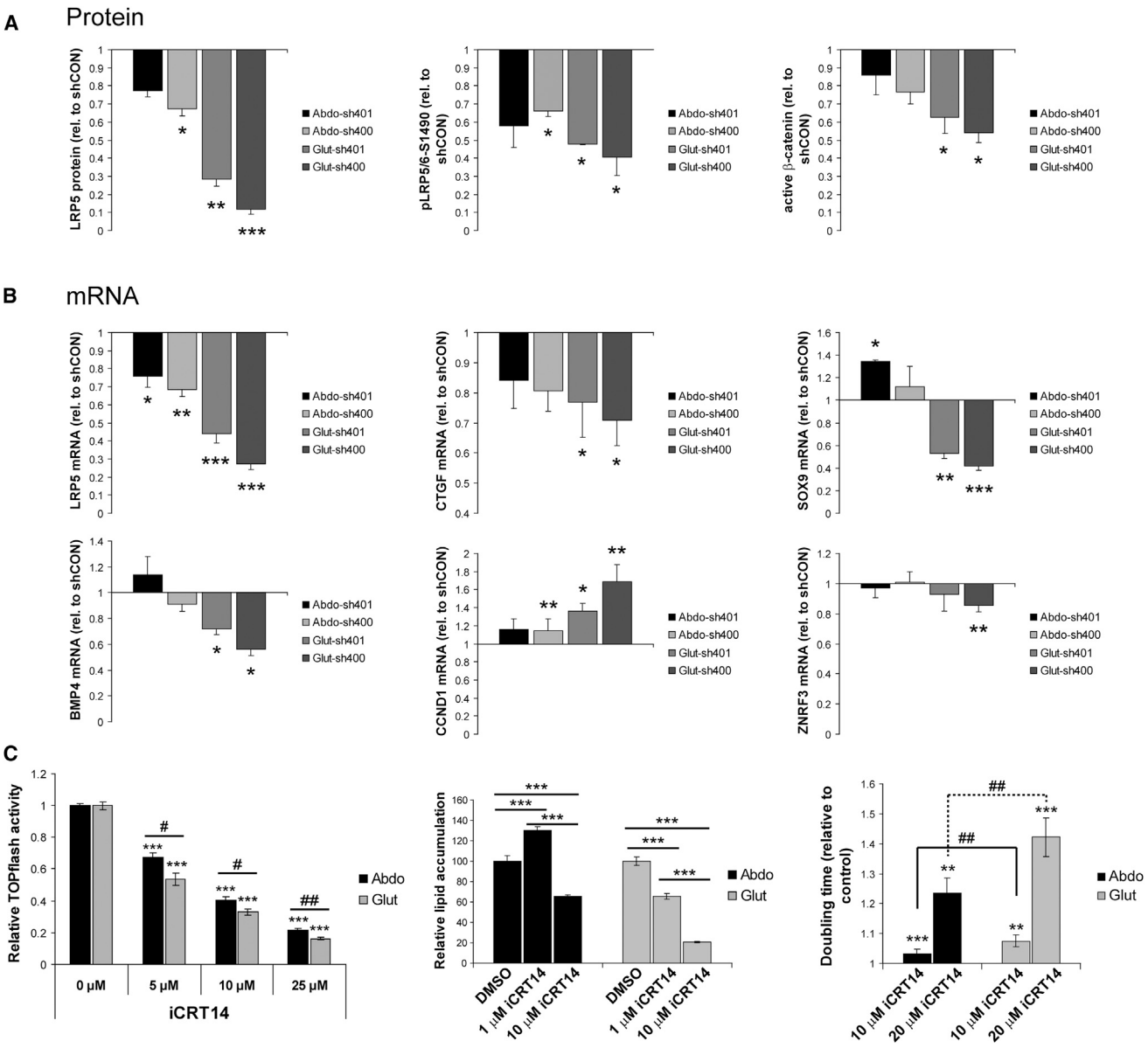

Figure 4. *LRP5*-KD in Abdominal and Gluteal SVCs Dose-Dependently Modulates β-Catenin Signaling

(A) Protein densitometry of LRP5, pLRP5/6-S1490, and active β-catenin in Abdo-sh401, Abdo-sh400, Glut-sh401, and Glut-sh400 SVCs. Densitometry data were normalized to α-tubulin and are shown relative to their respective shCON levels. n = 3–4 independent experiments.

(B) Gene expression profiling of β-catenin target genes in Abdo-sh401, Abdo-sh400, Glut-sh401, and Glut-sh400 SVCs. mRNA data were normalized to *18S* and are shown relative to their respective shCON levels. n = 4–7 independent experiments.

(C) Treatment with the β-catenin small-molecule inhibitor iCRT14 dose-dependently modulates TOPflash promoter activity, adipogenesis, and proliferation in immortalized abdominal and gluteal SVCs (n = 6–7 replicates). Histogram data are means ± SEM. $^{*,\#}p < 0.05$, $^{**,\#\#}p < 0.01$, $^{***}p < 0.001$. *,**,*** within group comparisons; $^{\#,\#\#}$ between group comparisons.

dose (10 μM) impaired differentiation, albeit to a lesser extent than the equivalent dose in gluteal cells. Accordingly, iCTR14-induced inhibition of β-catenin-dependent promoter activity was more pronounced in gluteal than abdominal SVCs. iCRT14 also dose-dependently impaired adipose progenitor proliferation. As expected, this effect was more marked in gluteal versus abdominal cells (Figure 4C). We conclude that the biological effects of *LRP5* KD in adipose progenitors are driven by dose-dependent reductions in β-catenin transcriptional activity, which, for an equivalent decrease in *LRP5* gene dosage, is more potently blocked in gluteal than abdominal SVCs.

DISCUSSION

Fat distribution is a heritable trait that strongly predicts diabetes and CVD risk independent of obesity. In this study we identify the

WNT co-receptor LRP5 as a regulator of adipose progenitor biology and regional adiposity. By examining three HBM pedigrees, we show that rare GoF *LRP5* mutations are associated with an increased amount of lower-body fat. Complimentary to these findings we also demonstrate, through the analysis of DXA data from > 3,000 individuals, that the minor allele of a common SNP in *LRP5* associated with low BMD correlates with modestly increased upper-body fat accumulation. From the direction of its effect upon BMD, this allele is likely to be associated with reduced LRP5 function. Based on our in vitro KD studies, the increased central adiposity observed in rs599083 minor allele carriers is likely to be driven by enhanced cellularity of the SC abdominal relative to the gluteofemoral fat depot. Nonetheless, in these same experiments, *LRP5*-KD SC abdominal SVCs exhibited impaired proliferation and enhanced inflammation. We speculate that this is likely to impact negatively on the size and quality of the SVC pool and ultimately adipocyte number in this depot, too, a hypothesis consistent with the histological analysis of SC abdominal WAT from a limited number of rs599083 minor versus homozygous major allele carriers (Figures S2B and S2C).

LRP5 HBM individuals also exhibited enhanced insulin sensitivity versus age-, gender-, and BMI-matched controls. This may be at least partly due to their more favorable body fat distribution coupled with greater WAT cellularity (i.e., fat storage capacity, thought to protect against ectopic lipid deposition and lipotoxicity) due to enhanced SVC proliferation and, in the case of gluteal SVCs, potentially also differentiation. In contrast, rs599083 was not associated with T2D risk or measures of BMI-adjusted insulin sensitivity in publically available data sets from the DIAGRAM (Morris et al., 2012) and MAGIC (Manning et al., 2012) consortia, respectively. However, power to detect phenotypic associations between WHR- and BMI-associated variants and related metabolic parameters can be low. Accordingly, not all signals associated with fat distribution showed significant associations with surrogates of insulin resistance in the meta-analysis by Heid et al. (Heid et al., 2010). This is likely due to the limited power to detect downstream phenotypes, given the relatively low effect sizes at individual loci, even when the overall phenotypic associations are strong.

The lack of and weak association between rs599083 and anthropometric measures of fat distribution in the OBB (Table S4) and GIANT data sets, respectively, is notable. In this regard we detected only modest age-, gender-, and BMI-adjusted correlations between anthropometric and DXA-derived measures of fat distribution within the OBB (Table S5). Furthermore, alterations in body shape and/or skeletal geometry consequent to the actions of LRP5 on bone may mask the associations between *LRP5* variants and anthropometric surrogates of adiposity. In keeping with this, rs3736228, a non-synonymous exonic SNP in *LRP5* that is in linkage disequilibrium with rs599083, was shown to modulate femoral neck width, femoral shaft geometry, and vertebral body size (Boudin et al., 2013; van Meurs et al., 2006). Moreover, in a study of 258 individuals with unexplained HBM, HBM cases had significantly broader skeletal frames compared with controls (Gregson et al., 2012). Accordingly, we detected no consistent differences in anthropometric measures of fat distribution between HBM *LRP5* mutation carriers and matched OBB controls (Table S2). Finally, distinct from the WAT expression pattern of *LRP5*, *RSPO3* (Figure 1C) and *ZNRF3* (Schleinitz et al., 2014) are more highly expressed in visceral versus SC fat. These contrasting gene expression profiles may also account for the more robust association between SNPs within these genes and body fat distribution in GWAS.

Much of the impetus for this work was based on an earlier search for WNT pathway genes that were differentially expressed between SC abdominal and gluteal SVCs. We had reasoned that these may underlie intrinsic differences in WNT pathway tone (signal strength) and/or specificity (canonical versus non-canonical pathway activation) between abdominal and gluteal progenitors. Such changes in turn might endow SVCs from these depots with distinct functional properties, thereby driving changes in fat distribution. As part of those analyses, *LRP5* was found to be more highly expressed in abdominal versus gluteal progenitors. Herein we show that, consistent with our original hypothesis, equivalent magnitude of *LRP5* KD in abdominal and gluteal SVCs leads to markedly different proportional reduction in LRP5 levels/activity and distinct biological outcomes; *LRP5* KD impaired proliferation to a greater extent in immortalized gluteal than abdominal progenitors (Figure 2B). Furthermore, while *LRP5* KD in gluteal SVCs led to impaired adipogenesis, differentiation in abdominal cells was unchanged and even enhanced following modest and low-level *LRP5* KD, respectively. Finally, compared with controls, gluteal but not abdominal *LRP5*-KD adipocytes were inflamed. We speculate that by modulating regional WAT cellularity, these diverse biological responses underlie, at least partly, the effects of LRP5 on fat distribution. Moreover, they are rooted in the different levels of *LRP5* expression between abdominal and gluteal progenitors coupled with dose-dependent effects of LRP5 on SVC function. As such, due to the lower *LRP5* transcript and protein levels in gluteal versus abdominal SVCs (Figures 1D and 1E), gluteal progenitors are likely to be more sensitive than abdominal progenitors to changes in (1) LRP5 function, due to missense variants, and (2) *LRP5* mRNA levels, e.g., decreased expression driven by obesity or intronic SNPs. In agreement with this hypothesis, we found that *LRP5* gene expression in gluteal but not SC abdominal WAT correlated negatively with upper-body fat accumulation in females (Table S8). Adipocyte size (an inverse correlate of WAT cellularity) has also been reported to be larger in the gluteal versus abdominal depot of women (Votruba and Jensen, 2007). Complicating the interpretation of this latter finding, however, hormonal signals—e.g., sex-steroids—can interact with WNT signaling tone in vivo to modulate adipocyte size (Elbers et al., 1999). Additionally, in weight-gaining adults, abdominal WAT is thought to expand by hypertrophy (Spalding et al., 2008; Tchoukalova et al., 2010) and gluteofemoral WAT by hyperplasia (Tchoukalova et al., 2010).

Mechanistically, the effects of *LRP5* KD on SVC proliferation arise from inhibition of canonical WNT signaling. This conclusion was confirmed by the dose-dependent decrease in both β-catenin-driven promoter activity and proliferation in adipose SVCs following treatment with iCTR14. Furthermore, the link between adipose cell inflammation and WNT/LRP5 signaling is likely to have its basis in the mutually antagonistic actions of the β-catenin and PCP pathways (Grumolato et al., 2010). Thus, suppressing canonical WNT signaling promotes JNK activation, thereby driving inflammation. Likewise, the enhanced differentiation seen in abdominal cells following low-level *LRP5*-KD is in

keeping with the well-established anti-adipogenic action of WNT/β-catenin signaling. In contrast, further reduction in LRP5 levels progressively restrains adipocyte differentiation. In line with this, *LRP5*-KD gluteal SVCs, which exhibit the lowest LRP5 protein levels, display a "paradoxical" block in adipogenesis. The anti-adipogenic actions of LRP5 deficiency are not mediated via altered non-canonical WNT signaling, as neither the PCP nor the WNT/Ca^{2+} pathways were differentially modulated in abdominal versus gluteal *LRP5*-KD cells. Moreover, in contrast to Palsgaard et al. (Palsgaard et al., 2012), we were unable to detect any changes in insulin/IGF1 pathway activity in response to *LRP5* KD (Figures 3B and S3G). Instead, utilizing iCRT14, we demonstrate that the anti-adipogenic effect of LRP5 deficiency is likely to be driven by impaired β-catenin transcriptional activity (Figure 4C). We note that we have not corroborated this conclusion by rescuing adipogenesis in *LRP5*-KD gluteal SVCs through augmenting β-catenin signaling. Such a rescue experiment, however, is technically challenging, since constitutively increasing β-catenin activity in adipose progenitors potently blocks adipogenesis (Christodoulides et al., 2009). Hence, rescuing differentiation in *LRP5*-KD gluteal cells would require precisely titrating the degree as well as the timing and duration of β-catenin signaling activation prior to and/or during differentiation. Our results suggest that, similar to its mode of action in stem/progenitor cells from other organs/tissues (Hirata et al., 2013; Kielman et al., 2002; Luis et al., 2011), canonical WNT signaling in human adipose SVCs is more complex than an on/off switch. Rather, it is associated with different biological outcomes dependent on a gradient of β-catenin transcriptional activity. Finally, in conjunction with earlier findings (Donati et al., 2014; Ross et al., 2000), our data also show that autonomous as well as non-autonomous WNT/β-catenin signals can both promote and inhibit adipogenesis.

In summary, we have established that LRP5 acts by titrating β-catenin signal strength to modulate adipose progenitor biology in a depot-specific manner, thus promoting lower-body fat accumulation. Rational manipulation of *LRP5* expression/activity to achieve a more beneficial pattern of fat distribution may offer a potential approach to treat obesity-associated CVD. We note in this respect that treatment with humanized antibodies against SOST (a secreted LRP5 antagonist) is currently in phase III trials for osteoporosis management (McClung and Grauer, 2014). Once such treatments become the mainstay for osteoporosis, it will be important to determine their effects on fat distribution and metabolic health.

EXPERIMENTAL PROCEDURES

Study Population and Sample Collection

Control study subjects were recruited from the OBB, a population-based collection of healthy subjects aged 30–50 years (http://www.oxfordbiobank.org.uk). HBM *LRP5* mutation carriers were recruited from the UK-based HBM study cohort (Gregson et al., 2012) (see Supplemental Information). Paired SC abdominal and gluteal WAT specimens were obtained by needle biopsy as described (McQuaid et al., 2011). Paired SC abdominal and visceral fat samples were obtained from patients undergoing elective surgery as part of the MolSURG study. All studies were approved by the Oxfordshire Clinical Research Ethics Committee and the Bath multi-centre Research Ethics Committee, and all volunteers gave written, informed consent. Other aspects of the study in pre- and post-menopausal women have previously been reported (Hodson et al., 2014).

Dual Energy X-Ray Absorptiometry

Whole-body DXAs were performed using a Lunar iDXA (GE Healthcare). Acquired images were processed using enCORE v14.1 software. Central-to-peripheral fat ratio was calculated as android fat (g) ÷ (arms + legs) fat (g).

Isolation, Culture, and Differentiation of Human SVCs

SVCs were isolated from WAT biopsies, cultured, and differentiated as described (Collins et al., 2010) (see Supplemental Information). SVCs isolated from a male subject were immortalized by co-expressing human telomerase reverse transcriptase and human papillomavirus type-16 E7 oncoprotein (Pinnick et al., 2014). To study the effects of iCRT14 (Sigma-Aldrich) on adipogenesis, SVCs were seeded in type I collagen-coated 96-well plates. Culture media were replaced after 24 hr with growth media containing iCRT14 (1 μM or 10 μM) or DMSO. Confluent cells were differentiated 48 hr later in the same concentration of iCRT14 (or DMSO) throughout for 21 days. Media were changed every 2–3 days. Intracellular lipid levels were quantified using the AdipoRed assay reagent (Lonza) and a CytoFluor Multi-Well Plate Reader series 4000 (PerSeptive Biosystems).

Estimation of Cell Doubling Time

Equal numbers of control and *LRP5*-KD SVCs, i.e., 400,000 or 150,000, were seeded in T175 and T75 flasks, respectively. Cells were trypsinized and double counted every 72 hr. Doubling time was calculated using the formula $T_d = (t_2 - t_1) \times [\log(2) \div \log(q_2 \div q_1)]$, where t = time (days) and q = cell number.

Lentiviral Constructs and Generation of Stable Cell Lines

MISSION *LRP5* shRNA and control plasmid DNA vectors were obtained from Sigma-Aldrich. The 7TFP WNT reporter lentiviral vector (Fuerer and Nusse, 2010) was obtained from Addgene. Lentiviral particles were produced by transient co-transfection of HEK293 cells with the vector of interest and packaging vectors (MISSION [Sigma-Aldrich] and ViraPower [Invitrogen] packaging mixes). Stable cell lines were generated by transduction of SVCs with lentiviral particles followed by selection in growth media containing 2 μg/ml puromycin.

Insulin Stimulation Studies of SVCs

Stimulation experiments with 10 nM or 100 nM insulin (Sigma-Aldrich) were performed as described (Palsgaard et al., 2012).

Genotyping, Quantitative Real-Time PCR, Western Blot Analyses, and Measurement of Adipocyte Size and Number

Genotyping and qRT-PCR were performed using TaqMan assays. Western blot analyses were performed using standard protocols. Adipocyte sizing was performed using a histological method. Full details are found in Supplemental Information.

Luciferase Reporter Assay

Immortalized SVCs stably expressing 7TFP were grown to confluence in type I collagen-coated 24-well plates in complete growth media, then treated with indicated concentrations of iCRT14 (or DMSO) in serum-free media for 24 hr. Cell lysates were harvested in passive lysis buffer, and reporter activity was measured using the Luciferase Assay System (Promega) and a Veritas Microplate Luminometer (Turner Biosystems). Data were normalized to protein concentration.

Statistical Analysis

Statistical analyses for association studies between *LRP5* SNPs and quantitative traits were performed using the PLINK program v.1.07 (http://pngu.mgh.harvard.edu/~purcell/plink/) (Purcell et al., 2007). All quantitative traits were log transformed and analyzed with a linear regression model. Data were adjusted for age, gender, and BMI. Significance is presented as empirical p values as calculated by the additional implementation of permutation procedures (default under PLINK) to the linear regression model. For parametric data, statistical significance was determined by pairwise comparisons using a two-tailed paired or unpaired Student's t test, as appropriate. For non-parametric data, group differences were determined using the Kruskal-Wallis one-way analysis of variance. Statistical significance was determined by pairwise comparisons using a two-tailed Mann-Whitney test. Statistical tests generating a $p < 0.05$ were considered significant. Partial correlations of

non-parametric data were performed using the SPSS Statistics software package and adjusted for age, gender, and BMI. For studies of the HBM cohort, matched analyses used radius matching based on age, gender, and BMI with a 3:1 ratio, using a multi-level regression model clustering by match set. All data are presented as means ± SEM unless otherwise stated.

SUPPLEMENTAL INFORMATION

Supplemental Information includes Supplemental Experimental Procedures, four figures, and eight tables and can be found with this article online at http://dx.doi.org/10.1016/j.cmet.2015.01.009.

AUTHOR CONTRIBUTIONS

N.Y.L. and C.C. designed and performed experiments, analyzed data, and co-wrote paper; M.J.N. analyzed genotyping data; K.M. undertook adipocyte sizing studies; S.A.H., J.H.T., and C.L.G. provided access to the HBM cohort; C.L.G. and E.L.D. undertook genotyping of the HBM cohort and analyzed data; B.A.F. and K.M. provided access to data and WAT from the pre- and post-menopausal women cohort; M.I.M. facilitated the generation of OBB exome chip array data and provided access to MolSURG WAT samples; F.K. provided access to the OBB, designed experiments, and co-wrote paper. All authors critically reviewed the manuscript.

ACKNOWLEDGMENTS

This research is supported by a Clinical Research Grant Programme from the European Foundation for the Study of Diabetes and a Project Grant from the British Heart Foundation (BHF) (PG/12/78/29862). K.M. is supported by the European Commission (FP7-PEOPLE-2011-IEF). The menopause study was funded by the BHF (PG/09/003). We are grateful to all the human volunteers and the CRU staff (L. Dennis, M. Gilbert, and J. Cheeseman in particular). We thank L. Hodson, co-investigator of the menopause study. We thank A. Clark for help with adipocyte histology. We thank K. Addison, J. Harris, G. Clark, and L. Wheeler for their careful sequencing, performed in the laboratory of Prof. M. Brown, with thanks. We are grateful to A. Sayers for writing the radius-matching Stata program used and S.K. Thomsen for helpful discussions.

Received: June 30, 2014
Revised: October 8, 2014
Accepted: January 14, 2015
Published: February 3, 2015

REFERENCES

Ai, M., Heeger, S., Bartels, C.F., and Schelling, D.K.; Osteoporosis-Pseudoglioma Collaborative Group (2005). Clinical and molecular findings in osteoporosis-pseudoglioma syndrome. Am. J. Hum. Genet. *77*, 741–753.

Alberti, K.G., Zimmet, P., and Shaw, J.; IDF Epidemiology Task Force Consensus Group (2005). The metabolic syndrome—a new worldwide definition. Lancet *366*, 1059–1062.

Billon, N., and Dani, C. (2012). Developmental origins of the adipocyte lineage: new insights from genetics and genomics studies. Stem Cell Rev. *8*, 55–66.

Boudin, E., Steenackers, E., de Freitas, F., Nielsen, T.L., Andersen, M., Brixen, K., Van Hul, W., and Piters, E. (2013). A common LRP4 haplotype is associated with bone mineral density and hip geometry in men-data from the Odense Androgen Study (OAS). Bone *53*, 414–420.

Boyden, L.M., Mao, J., Belsky, J., Mitzner, L., Farhi, A., Mitnick, M.A., Wu, D., Insogna, K., and Lifton, R.P. (2002). High bone density due to a mutation in LDL-receptor-related protein 5. N. Engl. J. Med. *346*, 1513–1521.

Christodoulides, C., Lagathu, C., Sethi, J.K., and Vidal-Puig, A. (2009). Adipogenesis and WNT signalling. Trends Endocrinol. Metab. *20*, 16–24.

Clevers, H., and Nusse, R. (2012). Wnt/β-catenin signaling and disease. Cell *149*, 1192–1205.

Collins, J.M., Neville, M.J., Hoppa, M.B., and Frayn, K.N. (2010). De novo lipogenesis and stearoyl-CoA desaturase are coordinately regulated in the human adipocyte and protect against palmitate-induced cell injury. J. Biol. Chem. *285*, 6044–6052.

Donati, G., Proserpio, V., Lichtenberger, B.M., Natsuga, K., Sinclair, R., Fujiwara, H., and Watt, F.M. (2014). Epidermal Wnt/β-catenin signaling regulates adipocyte differentiation via secretion of adipogenic factors. Proc. Natl. Acad. Sci. USA *111*, E1501–E1509.

Duncan, E.L., Danoy, P., Kemp, J.P., Leo, P.J., McCloskey, E., Nicholson, G.C., Eastell, R., Prince, R.L., Eisman, J.A., Jones, G., et al. (2011). Genome-wide association study using extreme truncate selection identifies novel genes affecting bone mineral density and fracture risk. PLoS Genet. *7*, e1001372.

Elbers, J.M., de Jong, S., Teerlink, T., Asscheman, H., Seidell, J.C., and Gooren, L.J. (1999). Changes in fat cell size and in vitro lipolytic activity of abdominal and gluteal adipocytes after a one-year cross-sex hormone administration in transsexuals. Metabolism *48*, 1371–1377.

Estrada, K., Styrkarsdottir, U., Evangelou, E., Hsu, Y.H., Duncan, E.L., Ntzani, E.E., Oei, L., Albagha, O.M., Amin, N., Kemp, J.P., et al. (2012). Genome-wide meta-analysis identifies 56 bone mineral density loci and reveals 14 loci associated with risk of fracture. Nat. Genet. *44*, 491–501.

Fontana, L., Eagon, J.C., Trujillo, M.E., Scherer, P.E., and Klein, S. (2007). Visceral fat adipokine secretion is associated with systemic inflammation in obese humans. Diabetes *56*, 1010–1013.

Fuerer, C., and Nusse, R. (2010). Lentiviral vectors to probe and manipulate the Wnt signaling pathway. PLoS ONE *5*, e9370.

Gesta, S., Blüher, M., Yamamoto, Y., Norris, A.W., Berndt, J., Kralisch, S., Boucher, J., Lewis, C., and Kahn, C.R. (2006). Evidence for a role of developmental genes in the origin of obesity and body fat distribution. Proc. Natl. Acad. Sci. USA *103*, 6676–6681.

Gong, Y., Slee, R.B., Fukai, N., Rawadi, G., Roman-Roman, S., Reginato, A.M., Wang, H., Cundy, T., Glorieux, F.H., Lev, D., et al.; Osteoporosis-Pseudoglioma Syndrome Collaborative Group (2001). LDL receptor-related protein 5 (LRP5) affects bone accrual and eye development. Cell *107*, 513–523.

Gonsalves, F.C., Klein, K., Carson, B.B., Katz, S., Ekas, L.A., Evans, S., Nagourney, R., Cardozo, T., Brown, A.M., and DasGupta, R. (2011). An RNAi-based chemical genetic screen identifies three small-molecule inhibitors of the Wnt/wingless signaling pathway. Proc. Natl. Acad. Sci. USA *108*, 5954–5963.

Gregson, C.L., Steel, S.A., O'Rourke, K.P., Allan, K., Ayuk, J., Bhalla, A., Clunie, G., Crabtree, N., Fogelman, I., Goodby, A., et al. (2012). 'Sink or swim': an evaluation of the clinical characteristics of individuals with high bone mass. Osteoporos. Int. *23*, 643–654.

Grumolato, L., Liu, G., Mong, P., Mudbhary, R., Biswas, R., Arroyave, R., Vijayakumar, S., Economides, A.N., and Aaronson, S.A. (2010). Canonical and noncanonical Wnts use a common mechanism to activate completely unrelated coreceptors. Genes Dev. *24*, 2517–2530.

Heid, I.M., Jackson, A.U., Randall, J.C., Winkler, T.W., Qi, L., Steinthorsdottir, V., Thorleifsson, G., Zillikens, M.C., Speliotes, E.K., Mägi, R., et al.; MAGIC (2010). Meta-analysis identifies 13 new loci associated with waist-hip ratio and reveals sexual dimorphism in the genetic basis of fat distribution. Nat. Genet. *42*, 949–960.

Hirata, A., Utikal, J., Yamashita, S., Aoki, H., Watanabe, A., Yamamoto, T., Okano, H., Bardeesy, N., Kunisada, T., Ushijima, T., et al. (2013). Dose-dependent roles for canonical Wnt signalling in de novo crypt formation and cell cycle properties of the colonic epithelium. Development *140*, 66–75.

Hodson, L., Harnden, K., Banerjee, R., Real, B., Marinou, K., Karpe, F., and Fielding, B.A. (2014). Lower resting and total energy expenditure in postmenopausal compared with premenopausal women matched for abdominal obesity. J Nutr Sci *3*, e3.

Jensen, M.D. (2008). Role of body fat distribution and the metabolic complications of obesity. J. Clin. Endocrinol. Metab. *93* (1), S57–S63.

Karpe, F., and Pinnick, K.E. (2014). Biology of upper-body and lower-body adipose tissue-link to whole-body phenotypes. Nat. Rev. Endocrinol. Published online November 4, 2014. http://dx.doi.org/10.1038/nrendo.2014.185.

Kielman, M.F., Rindapää, M., Gaspar, C., van Poppel, N., Breukel, C., van Leeuwen, S., Taketo, M.M., Roberts, S., Smits, R., and Fodde, R. (2002). Apc modulates embryonic stem-cell differentiation by controlling the dosage of beta-catenin signaling. Nat. Genet. *32*, 594–605.

Krishnan, V., Bryant, H.U., and Macdougald, O.A. (2006). Regulation of bone mass by Wnt signaling. J. Clin. Invest. *116*, 1202–1209.

Little, R.D., Carulli, J.P., Del Mastro, R.G., Dupuis, J., Osborne, M., Folz, C., Manning, S.P., Swain, P.M., Zhao, S.C., Eustace, B., et al. (2002). A mutation in the LDL receptor-related protein 5 gene results in the autosomal dominant high-bone-mass trait. Am. J. Hum. Genet. *70*, 11–19.

Luis, T.C., Naber, B.A., Roozen, P.P., Brugman, M.H., de Haas, E.F., Ghazvini, M., Fibbe, W.E., van Dongen, J.J., Fodde, R., and Staal, F.J. (2011). Canonical wnt signaling regulates hematopoiesis in a dosage-dependent fashion. Cell Stem Cell *9*, 345–356.

Mani, A., Radhakrishnan, J., Wang, H., Mani, A., Mani, M.A., Nelson-Williams, C., Carew, K.S., Mane, S., Najmabadi, H., Wu, D., and Lifton, R.P. (2007). LRP6 mutation in a family with early coronary disease and metabolic risk factors. Science *315*, 1278–1282.

Manning, A.K., Hivert, M.F., Scott, R.A., Grimsby, J.L., Bouatia-Naji, N., Chen, H., Rybin, D., Liu, C.T., Bielak, L.F., Prokopenko, I., et al.; DIAbetes Genetics Replication And Meta-analysis (DIAGRAM) Consortium; Multiple Tissue Human Expression Resource (MUTHER) Consortium (2012). A genome-wide approach accounting for body mass index identifies genetic variants influencing fasting glycemic traits and insulin resistance. Nat. Genet. *44*, 659–669.

McClung, M.R., and Grauer, A. (2014). Romosozumab in postmenopausal women with osteopenia. N. Engl. J. Med. *370*, 1664–1665.

McQuaid, S.E., Hodson, L., Neville, M.J., Dennis, A.L., Cheeseman, J., Humphreys, S.M., Ruge, T., Gilbert, M., Fielding, B.A., Frayn, K.N., and Karpe, F. (2011). Downregulation of adipose tissue fatty acid trafficking in obesity: a driver for ectopic fat deposition? Diabetes *60*, 47–55.

Morris, A.P., Voight, B.F., Teslovich, T.M., Ferreira, T., Segrè, A.V., Steinthorsdottir, V., Strawbridge, R.J., Khan, H., Grallert, H., Mahajan, A., et al.; Wellcome Trust Case Control Consortium; Meta-Analyses of Glucose and Insulin-related traits Consortium (MAGIC) Investigators; Genetic Investigation of ANthropometric Traits (GIANT) Consortium; Asian Genetic Epidemiology Network–Type 2 Diabetes (AGEN-T2D) Consortium; South Asian Type 2 Diabetes (SAT2D) Consortium; DIAbetes Genetics Replication And Meta-analysis (DIAGRAM) Consortium (2012). Large-scale association analysis provides insights into the genetic architecture and pathophysiology of type 2 diabetes. Nat. Genet. *44*, 981–990.

Palsgaard, J., Emanuelli, B., Winnay, J.N., Sumara, G., Karsenty, G., and Kahn, C.R. (2012). Cross-talk between insulin and Wnt signaling in preadipocytes: role of Wnt co-receptor low density lipoprotein receptor-related protein-5 (LRP5). J. Biol. Chem. *287*, 12016–12026.

Pinnick, K.E., Nicholson, G., Manolopoulos, K.N., McQuaid, S.E., Valet, P., Frayn, K.N., Denton, N., Min, J.L., Zondervan, K.T., Fleckner, J., et al.; MolPAGE Consortium (2014). Distinct developmental profile of lower-body adipose tissue defines resistance against obesity-associated metabolic complications. Diabetes *63*, 3785–3797.

Purcell, S., Neale, B., Todd-Brown, K., Thomas, L., Ferreira, M.A.R., Bender, D., Maller, J., Sklar, P., de Bakker, P.I.W., Daly, M.J., and Sham, P.C. (2007). PLINK: a tool set for whole-genome association and population-based linkage analyses. Am. J. Hum. Genet. *81*, 559–575.

Qatanani, M., and Lazar, M.A. (2007). Mechanisms of obesity-associated insulin resistance: many choices on the menu. Genes Dev. *21*, 1443–1455.

Randall, J.C., Winkler, T.W., Kutalik, Z., Berndt, S.I., Jackson, A.U., Monda, K.L., Kilpeläinen, T.O., Esko, T., Mägi, R., Li, S., et al.; DIAGRAM Consortium; MAGIC Investigators (2013). Sex-stratified genome-wide association studies including 270,000 individuals show sexual dimorphism in genetic loci for anthropometric traits. PLoS Genet. *9*, e1003500.

Rivadeneira, F., Styrkársdottir, U., Estrada, K., Halldórsson, B.V., Hsu, Y.H., Richards, J.B., Zillikens, M.C., Kavvoura, F.K., Amin, N., Aulchenko, Y.S., et al.; Genetic Factors for Osteoporosis (GEFOS) Consortium (2009). Twenty bone-mineral-density loci identified by large-scale meta-analysis of genome-wide association studies. Nat. Genet. *41*, 1199–1206.

Ross, S.E., Hemati, N., Longo, K.A., Bennett, C.N., Lucas, P.C., Erickson, R.L., and MacDougald, O.A. (2000). Inhibition of adipogenesis by Wnt signaling. Science *289*, 950–953.

Saarinen, A., Saukkonen, T., Kivelä, T., Lahtinen, U., Laine, C., Somer, M., Toiviainen-Salo, S., Cole, W.G., Lehesjoki, A.E., and Mäkitie, O. (2010). Low density lipoprotein receptor-related protein 5 (LRP5) mutations and osteoporosis, impaired glucose metabolism and hypercholesterolaemia. Clin. Endocrinol. (Oxf.) *72*, 481–488.

Schenk, S., Saberi, M., and Olefsky, J.M. (2008). Insulin sensitivity: modulation by nutrients and inflammation. J. Clin. Invest. *118*, 2992–3002.

Schleinitz, D., Klöting, N., Lindgren, C.M., Breitfeld, J., Dietrich, A., Schön, M.R., Lohmann, T., Dreßler, M., Stumvoll, M., McCarthy, M.I., et al. (2014). Fat depot-specific mRNA expression of novel loci associated with waist-hip ratio. Int J Obes (Lond) *38*, 120–125.

Semple, R.K., Savage, D.B., Cochran, E.K., Gorden, P., and O'Rahilly, S. (2011). Genetic syndromes of severe insulin resistance. Endocr. Rev. *32*, 498–514.

Singh, R., Smith, E., Fathzadeh, M., Liu, W., Go, G.W., Subrahmanyan, L., Faramarzi, S., McKenna, W., and Mani, A. (2013). Rare nonconservative LRP6 mutations are associated with metabolic syndrome. Hum. Mutat. *34*, 1221–1225.

Spalding, K.L., Arner, E., Westermark, P.O., Bernard, S., Buchholz, B.A., Bergmann, O., Blomqvist, L., Hoffstedt, J., Näslund, E., Britton, T., et al. (2008). Dynamics of fat cell turnover in humans. Nature *453*, 783–787.

Tchkonia, T., Giorgadze, N., Pirtskhalava, T., Thomou, T., DePonte, M., Koo, A., Forse, R.A., Chinnappan, D., Martin-Ruiz, C., von Zglinicki, T., and Kirkland, J.L. (2006). Fat depot-specific characteristics are retained in strains derived from single human preadipocytes. Diabetes *55*, 2571–2578.

Tchkonia, T., Lenburg, M., Thomou, T., Giorgadze, N., Frampton, G., Pirtskhalava, T., Cartwright, A., Cartwright, M., Flanagan, J., Karagiannides, I., et al. (2007). Identification of depot-specific human fat cell progenitors through distinct expression profiles and developmental gene patterns. Am. J. Physiol. Endocrinol. Metab. *292*, E298–E307.

Tchoukalova, Y.D., Votruba, S.B., Tchkonia, T., Giorgadze, N., Kirkland, J.L., and Jensen, M.D. (2010). Regional differences in cellular mechanisms of adipose tissue gain with overfeeding. Proc. Natl. Acad. Sci. USA *107*, 18226–18231.

Turer, A.T., Khera, A., Ayers, C.R., Turer, C.B., Grundy, S.M., Vega, G.L., and Scherer, P.E. (2011). Adipose tissue mass and location affect circulating adiponectin levels. Diabetologia *54*, 2515–2524.

van Meurs, J.B., Rivadeneira, F., Jhamai, M., Hugens, W., Hofman, A., van Leeuwen, J.P., Pols, H.A., and Uitterlinden, A.G. (2006). Common genetic variation of the low-density lipoprotein receptor-related protein 5 and 6 genes determines fracture risk in elderly white men. J. Bone Miner. Res. *21*, 141–150.

Votruba, S.B., and Jensen, M.D. (2007). Sex differences in abdominal, gluteal, and thigh LPL activity. Am. J. Physiol. Endocrinol. Metab. *292*, E1823–E1828.

Weidinger, G., and Moon, R.T. (2003). When Wnts antagonize Wnts. J. Cell Biol. *162*, 753–755.

Yusuf, S., Hawken, S., Ounpuu, S., Bautista, L., Franzosi, M.G., Commerford, P., Lang, C.C., Rumboldt, Z., Onen, C.L., Lisheng, L., et al.; INTERHEART Study Investigators (2005). Obesity and the risk of myocardial infarction in 27,000 participants from 52 countries: a case-control study. Lancet *366*, 1640–1649.

Cell Metabolism, Volume *21*

Supplemental Information

LRP5 Regulates Human Body Fat Distribution by Modulating Adipose Progenitor Biology in a Dose- and Depot-Specific Fashion

Nellie Y. Loh, Matt J. Neville, Kyriakoula Marinou, Sarah A. Hardcastle, Barbara A. Fielding, Emma L. Duncan, Mark I. McCarthy, Jonathan H. Tobias, Celia L. Gregson, Fredrik Karpe, and Constantinos Christodoulides

Supplemental Information

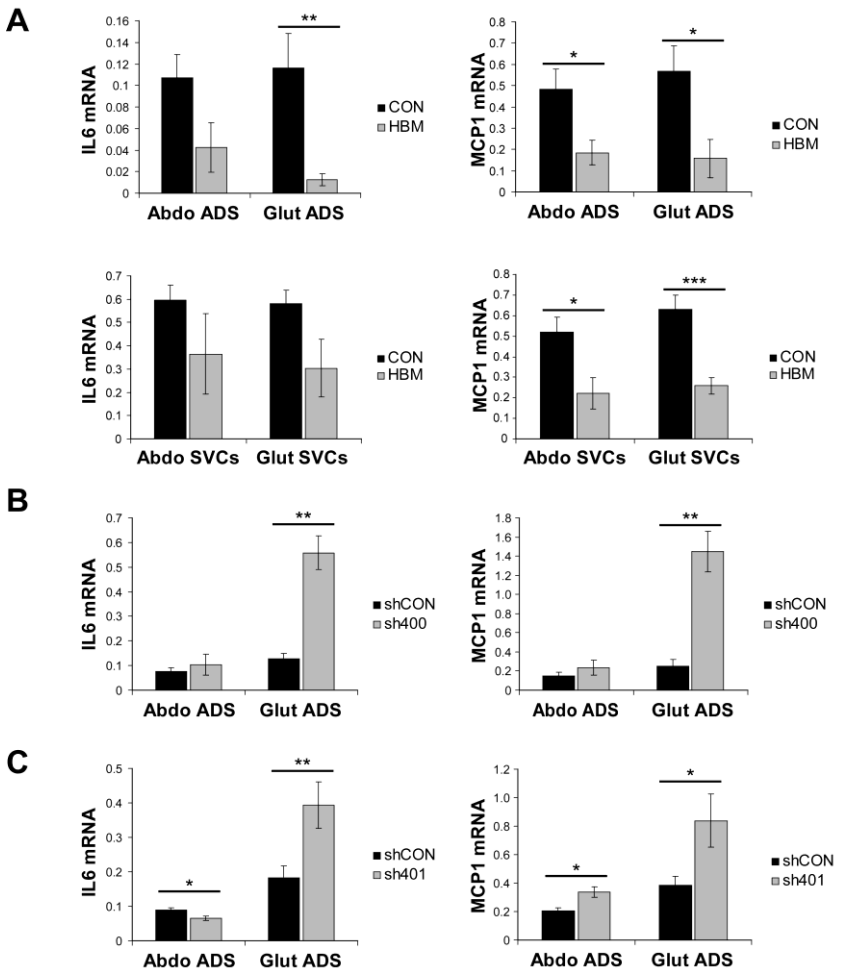

Figure S1 (Relates to Table 1 and Figure 2) Cellular inflammation in fractionated SC WAT of HBM *LRP5* mutation carriers, and *in vitro*-differentiated *LRP5* kd adipocytes. qRT-PCR analyses of *IL6* and *MCP1*, two markers of inflammation, in abdominal and gluteal (**A**) mature adipocytes (ADS) and SVCs isolated from WAT biopsies of subjects with HBM-causing gain-of-function *LRP5* mutations (n=4) and normal controls (n=24 for ADS, n=25 for SVCs), and (**B**) sh400 and (**C**) sh401 cells, and their respective controls, following 14 days of *in vitro* adipogenesis (n=4-7 independent experiments). qRT-PCR data were normalised to *18S*. *p<0.05, **p<0.01, ***p<0.001. Histogram data are expressed as means ± SEM.

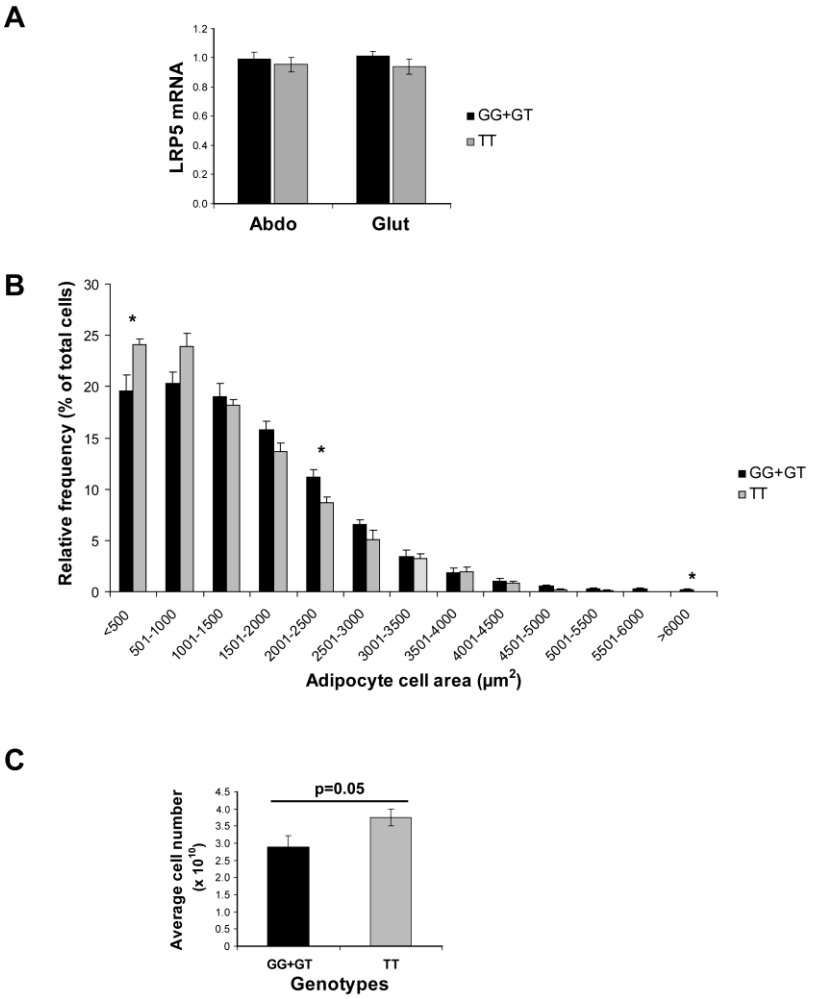

Figure S2 (Relates to Table 3) Comparison of *LRP5* mRNA levels in SC abdominal and gluteal WAT, and adipocyte cell size and number in abdominal SC WAT of subjects grouped according to their rs599083 genotype. (**A**) *LRP5* mRNA levels in SC abdominal and gluteal WAT from carriers of the low BMD-associated, minor allele (GG and GT; n=12 lean, 10 obese) *vs*. individuals homozygous for the common allele (TT; n=7 lean, 8 obese) at rs599083. qRT-PCR data were normalised to *PPIA* and *PGK1*. (**B-C**) Relative frequency of adipocytes of different sizes (cross sectional area, μm^2) (**B**), and estimated total adipocyte number in the android region (**C**) in carriers of the low BMD-associated allele (GG and GT; n=13) *vs.* individuals homozygous for the common allele (TT; n=5) at rs599083. >250 adipocytes were measured for each biopsy. Subject characteristics are shown in **Table S3**. *p<0.05. Histogram data are expressed as means ± SEM.

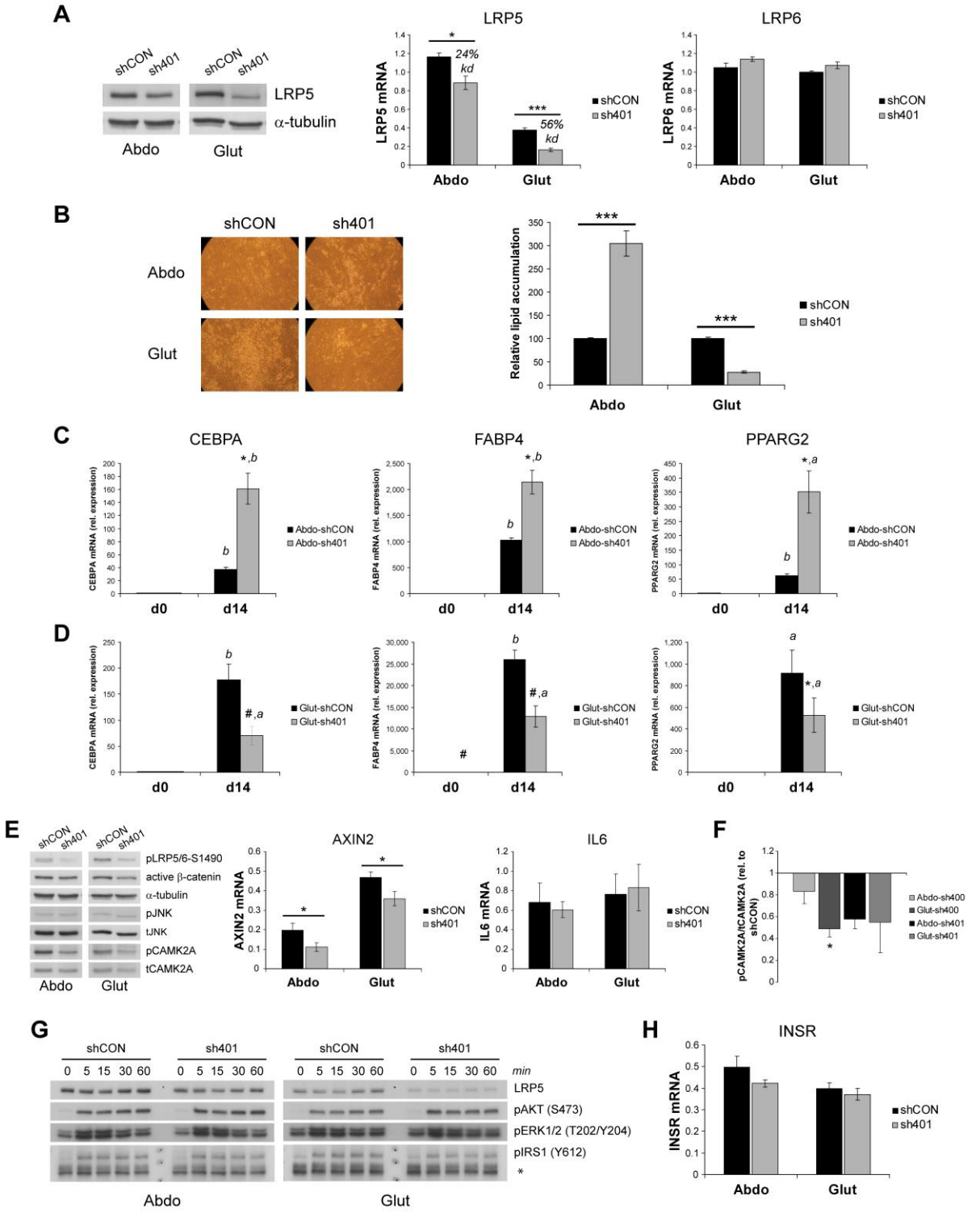

Figure S3 (Relates to Figures 2 and 3) Effects of *LRP5* kd in immortalised abdominal and gluteal SVCs on adipogenesis, and WNT and insulin signalling pathways. (**A**) *LRP5* kd was confirmed by Western blot and qRT-PCR analyses. *LRP5* mRNA levels were reduced by an

average of 24% and 56% in Abdo-sh401 and Glut-sh401 SVCs, respectively, compared with their respective control cells. *LRP6* gene expression was not significantly altered by *LRP5* kd with sh401. shCON=control, sh401=*LRP5* kd cells. α-tubulin was used as a Western blot loading control. *p<0.05, ***p<0.001. (**B**) Representative micrographs of shCON and sh401 abdominal and gluteal precursors at day 14 of adipogenic differentiation. Histogram shows relative lipid accumulation as assessed by AdipoRed assay (n=22-24). ***p<0.001. (**C-D**) Relative mRNA expression of adipogenic genes *CEBPA*, *FABP4* and *PPARG2* in (**C**) abdominal, and (**D**) gluteal cells at baseline (d0) and day 14 (d14) of adipogenic differentiation. shCON *vs*. sh401 cells: *p<0.05, $^{\#}$p<0.01; d0 *vs.* d14 cells: ^{a}p<0.05, ^{b}p<0.01. (**E**) Western blots for phospho-LRP5/6 (Ser1490) (pLRP5/6-S1490), active β-catenin, pJNK, and pCAMK2A, and qRT-PCR analyses of *AXIN2* and *IL6*, in shCON and sh401 abdominal and gluteal SVCs. α-tubulin, total-JNK (tJNK) and total CAMK2A (tCAMK2A) were used as loading controls for Western blots. *p<0.05. (**F**) Protein densitometry of pCAMK2A/tCAMK2A in Abdo-sh400, Glut-sh400, Abdo-sh401 and Glut-sh401 SVCs. Densitometry data are shown relative to their respective shCON levels. N=3 independent experiments. *p<0.05. (**G**) Representative Western blots of confluent shCON and sh401 abdominal and gluteal SVCs stimulated with 100 nM insulin for indicated length of time. *non-specific band, used as loading control. (**H**) Insulin receptor (*INSR*) mRNA levels in control and sh401 abdominal and gluteal SVCs. qRT-PCR data were normalised to *18S*. Histogram data are expressed as means ± SEM. N=4 independent experiments.

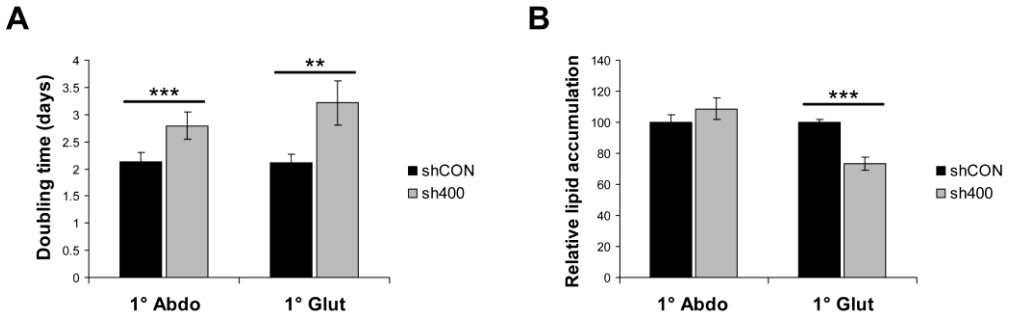

Figure S4 (Relates to Figure 2) Effects of *LRP5* kd in primary SC abdominal and gluteal SVCs on proliferation and adipogenesis. (**A**) Doubling time of control (shCON) and *LRP5* kd (sh400) abdominal and gluteal primary SVCs (n=11). (**B**) Relative lipid accumulation in differentiation day 21 shCON and sh400 primary abdominal and gluteal cells (n=16). **p<0.01, ***p<0.001. Histogram data are expressed as means ± SEM.

Table S1. (Relates to Table 2) Anthropometry and DXA-derived measures of body fat distribution of HBM subjects with gain-of-function *LRP5* mutations *vs.* the rest of the (non-*LRP5*) HBM cohort.

	Unadjusted Means ± SD		**Adjusted for gender, age and BMI Mean (95% CI)**	
	***LRP5* HBM (n=6)**	**non-*LRP5* HBM (n=134)**	***LRP5* HBM**	**non-*LRP5* HBM**
Age (yrs)	43.0 ± 14.5	60.1 ± 14.0		
BMI (kg/m^2)	27.7 ± 4.3	30.8 ± 6.0		
Tissue legs, % fat	39.5 ± 11.8	40.5 ± 9.6	41.2 (36.6, 45.7)	36.4 (35.4, 37.4)[a]
Tissue android, % fat	37.6 ± 14.7	48.6 ± 8.3	40.0 (35.2, 44.9)	46.3 (45.2, 47.4)[a]
Android:leg fat ratio (%)	19.0 ± 4.8	31.9 ± 10.8	21.9 (14.5, 29.3)	34.1 (32.4, 35.7)[b]
Android:total fat ratio (%)	7.1 ± 1.6	9.3 ± 1.6	7.6 (6.5, 8.6)	9.5 (9.3, 9.8)[c]
Central:peripheral fat mass ratio (g/g)	15.0 ± 3.9	22.8 ± 7.4	16.7 (11.8, 21.6)	24.6 (23.5, 25.7)[b]

Non-*LRP5* HBM group of 134 represents all HBM cases (indexes/relatives/spouses) with BMD Z-score of: (a) ≥+3.2 for total hip and ≥+1.2 for L1, or (b) ≥ +3.2 for L1 and ≥+1.2 for total hip (Gregson et al., 2013). 4 (66.7%) *LRP5* HBM and 112 (83.6%) non-*LRP5* HBM subjects were female. The p-values represent the strength of evidence against the H_o that non-*LRP5* HBM have same variable measures as *LRP5* HBM. [a]p<0.05, [b]p<0.01, [c]p<0.001. Abbreviations: HBM, high bone mass; CI, confidence interval; BMI, body mass index.

Table S2. (Relates to Table 1) Additional anthropometry and plasma biochemistry data from HBM patients with *LRP5* gain-of-function mutations *vs*. age-, gender-, and BMI-matched OBB controls.

	S1	Controls for S1	S2	Controls for S2	S3	Controls for S3	S4	Controls for S4	S5	Controls for S5	S6	Controls for S6
n		129 (77[a])		74 (42[a])		105 (65[a])		51 (33[a])		55 (33[a])		102 (59[a])
Age (yrs)	45	44.8 (44.3-45.2)	**68**	49.1 (48.9-49.3)	**50**	48.0 (47.7-48.4)	**28**	31.9 (31.5-32.2)	38	38.1 (36.9-39.3)	**34**	34.6 (34.1-35.1)
Gender	F	F	F	F	F	F	M	M	F	F	M	M
Waist circumference (cm)	**89**	86 (84-87)	**92**	87 (85-88)	84	85 (84-86)	**74**	81 (80-82)	**109**	104 (102-106)	**105**	97 (96-98)
Hip circumference (cm)	105	104 (103-105)	**99**	105 (104-106)	**99**	102 (101-103)	90	93 (89-97)	**124**	118 (117-120)	**116**	105 (104-106)
WHR	**0.85**	0.82 (0.81-0.83)	**0.93**	0.82 (0.81-0.84)	0.85	0.83 (0.82-0.85)	**0.82**	0.85 (0.84-0.86)	0.88	0.88 (0.86-0.90)	0.91	0.92 (0.91-0.93)
Plasma glucose (mmol/liter)	**4.6**	5.1 (5.1-5.2)	5.2	5.1 (5.0-5.2)	**5.4**	5.2 (5.1-5.3)	**4.4**	5.2 (5.1-5.3)	**4.6**	5.3 (5.1-5.4)	**5.0**	5.4 (5.3-5.5)
Plasma insulin (mU/liter)	**5.1**	12.8 (12.0-13.6)	13.0	13.4 (12.1-14.6)	**11.9**	12.9 (12.2-13.7)	**5.1**	11.4 (10.3-12.5)	**9.9**	18.9 (16.7-21.1)	**9.8**	16.6 (15.2-17.9)

Data for controls are means (95% CI). Values below/above the 95% CI in bold. *n*, number of age-, gender-, and BMI-matched controls. [a]number of controls with DXA measurements. Subjects from Kindred 1 (S1, S2) and Kindred 2 (S3, S4) carry the A242T mutation, those from Kindred 3 (S5, S6) carry the N198S mutation. NB. We were unable to match subjects S2 and S4 for age. Abbreviations: HBM, high bone mass; CI, confidence interval; WHR, waist-to-hip ratio.

Table S3. (Relates to Table 3) Anthropometry of **Figure S2B-C** subjects, grouped according to their rs599083 genotype.

	GG+GT	**TT**	***P***
n	13	5	
Gender	8M, 5F	3M, 2F	
Age (yrs)	40.5 ± 6.1	45.4 ± 1.5	0.1
BMI (kg/m^2)	33.8 ± 4.9	36.5 ± 3.0	0.1
Android fat mass (g)	4116 ± 1493	4754 ± 970	0.1

Abbreviations: BMI, body mass index. Data are means ± SD. *P* = p-value, two-tailed Mann Whitney test.

Table S4. (Relates to Table 3) Association studies between rs599083 and anthropometric measures of body fat distribution of subjects from the Oxford Biobank, adjusted for age, gender, and BMI.

	rs599083 **EA=G, EAF=0.34**		
Trait	***p-value***	***β***	***N***
Waist circumference (cm)	0.5	-0.005	5,573
Hip circumference (cm)	0.8	-0.006	5,572
WHR	0.7	0.005	5,571

Abbreviations: BMI, body mass index; WHR, waist-to-hip ratio; EA, effect allele; EAF, effect allele frequency. *P*-value, empirical p-value. β = standardised beta value. *N* = number of subjects. Data from 2,468 men and 3,105 women.

Table S5. (Relates to Table 3) Partial correlations between anthropometric and DXA-derived measures of body fat distribution of subjects from the Oxford Biobank, adjusted for age, gender, and BMI.

Traits	***rho***	***N***
WHR *vs.* android/gynoid	0.54	3,394
WHR *vs*. android/leg	0.49	3,394
Waist *vs*. android fat (g)	0.54	3,394
Waist *vs*. visceral fat (g)	0.46	3,381
Hip *vs*. gynoid fat (g)	0.53	3,395
Hip *vs*. leg fat (g)	0.46	3,395

Abbreviations: BMI, body mass index; WHR, waist-to-hip ratio. *rho,* Spearman's correlation coefficient. *N* = number of subjects. Data from 1,477 men and 1,918 women.

Table S6. (Relates to Figure 1) Anthropometry and plasma biochemistry of 20 lean and 20 obese male and female subjects from the Oxford Biobank.

	Lean	**Obese**	***P***
n	20	20	
Age (yrs)	44.3 ± 5.6	43.0 ± 4.3	0.363
BMI (kg/m^2)	23.4 ± 1.4	33.6 ± 5.3	<0.001
Waist circumference (cm)	83.0 ± 7.9	110.2 ± 14.0	<0.001
Hip circumference (cm)	97.6 ± 3.6	115.4 ± 9.2	<0.001
Plasma glucose (mmol/liter)	5.1 ± 0.5	5.4 ± 0.6	0.147
Plasma insulin (mU/liter)	8.5 ± 2.9	17.2 ± 8.5	<0.001
Triglycerides (mmol/liter)	1.2 ± 1.1	1.7 ± 0.8	<0.001
Plasma HDL cholesterol (mmol/liter)	1.3 ± 0.3	1.1 ± 0.3	0.013

Data are means ± SD. *P* = p-value for lean *vs.* obese subjects, two-tailed Mann Whitney test. 50% of lean and 50% obese subjects were women. Abbreviations: BMI, body mass index; HDL, high-density lipoprotein.

Table S7. (Relates to Figure 1) Anthropometry and plasma biochemistry in pre- and post-menopausal females recruited according to waist circumference.

	WC<80cm	**WC≥80**	***P***
n	23	24	
Age (yrs)	51.0 ± 9.4	50.8 ± 8.8	0.89
BMI (kg/m^2)	23.2 ± 1.8	26.2 ± 2.3	<0.0001
Waist circumference (cm)	76.0 ± 2.9	88.3 ± 6.7	<0.0001
Hip circumference (cm)	94.8 ± 4.0	101.5 ± 6.1	0.0001
Plasma glucose (mmol/liter)	4.8 ± 0.3	5.0 ± 0.4	0.04
Plasma insulin (mU/liter)	9.9 ± 3.5	11.0 ± 2.7	0.1
Triglycerides (mmol/liter)	809 ± 304	893 ± 439	0.6
Plasma HDL cholesterol (mmol/liter)	1.8 ± 0.4	1.6 ± 0.3	0.06

Data are means ± SD. *P* = p-value for women with WC<80cm *vs.* women with WC≥80cm, two-tailed Mann Whitney test. Abbreviations: WC, waist circumference; BMI, body mass index; HDL, high-density lipoprotein. Ten women per group were pre-menopausal.

Table S8. (Relates to Figure 1) Partial correlations (Spearman's) of *LRP5* mRNA levels in SC abdominal and gluteal WAT with measures of body fat distribution, plasma chemistry and markers of inflammation in the pre- and post-menopausal female cohort (n=47), adjusted for age, BMI, and menopause status.

	Abdominal		**Gluteal**	
Traits	***rho***	***P***	***rho***	***P***
Android fat[a]	0.17	0.3	-0.34	**0.02**
Gynoid fat[a]	0.28	0.07	0.17	0.3
Android:gynoid	0.09	0.6	-0.39	**0.01**
Visceral fat[b]	0.16	0.3	-0.31	**0.04**
Subcut. fat[b]	0.36	**0.02**	0.01	0.9
VAT:SCAT	-0.06	0.7	-0.31	**0.04**
WHR	-0.16	0.3	-0.20	0.2
Waist (cm)	-0.04	0.8	-0.29	0.06
Hip (cm)	0.30	**0.05**	-0.06	0.7
Insulin[c]	-0.19	0.2	-0.57	**<0.0001**
HOMA-IR	-0.12	0.4	-0.53	**<0.0001**
Log CRP[c]	-0.05	0.7	-0.32	**0.04**
MCP1[d]	-0.12	0.4	-0.35	**0.02**
CD68[d]	0.09	0.6	-0.33	**0.03**

Abbreviations: BMI, body mass index; subcut., subcutaneous; VAT, visceral adipose tissue; SCAT, subcutaneous adipose tissue; HOMA-IR, Homeostasis Model Assessment-estimated Insulin Resistance; CRP, C-reactive protein; MCP1, monocyte chemotactic protein 1. Measurements determined by [a]DXA/[b]MRI/[c]plasma chemistry/[d]qRT-PCR. Significant p-values in bold.

Supplemental Experimental Procedures

High bone mass (HBM) subjects carrying *LRP5* mutations: The HBM study is a UK-based multi-centered observational study of adults with unexplained HBM identified by screening 335,115 DXA scans from 13 UK DXA databases from which 258 HBM probands with BMD Z-score ≥+3.2 were identified. All participants were clinically assessed by one doctor using a standardized structured history and examination questionnaire, after which total-body Lunar prodigy DXA scans were performed (Gregson et al., 2013; Gregson et al., 2012). Written informed consent was collected for all, in line with the Declaration of Helsinki. Participants were excluded if they were aged <18 years, pregnant, or unable to provide written informed consent for any reason. This study was approved by the Bath Multicenter Research Ethics Committee (REC) and at each NHS Local REC. Cases with HBM *LRP5* mutations were identified by targeted sequencing of exons 2-4 of *LRP5* (i.e. the sites of previously described HBM cases). Primers are available upon request (Duncan et al., 2009). Six autosomal dominant HBM cases from 3 kindreds participated in the follow-on study. All subjects underwent basic anthropometric measurements, fasting blood sampling and a DXA scan. Lunar measured body composition parameters were compared between 6 *LRP5* HBM cases and 18 matched non-*LRP5* HBM controls.

Genotyping: Subjects were genotyped using TaqMan® SNP Genotyping Assays as previously described (Vasan et al., 2011).

Isolation, culture, and differentiation of human SVCs: The SVC layer containing preadipocytes was separated from mature adipocytes following collagenase (Roche)-digestion (1 mg/ml in Hanks' buffered salt solution) of WAT biopsies, and cultured in Dulbecco's modified Eagle's medium nutrient mixture F-12 Ham (DMEM-F12) supplemented with 10% foetal calf serum (FCS), 2 mM L-glutamine, 0.25 ng/ml fibroblast growth factor, 100 units/ml penicillin and 100 μg/ml streptomycin, as previously described (Collins et al., 2010).

For differentiation experiments, SVCs were grown to confluence in 6-well plates, and stimulated for 14 days with a standard adipogenic medium (DMEM-F12 containing 2mM glutamine, 17 μM pantothenate, 100 nM human insulin, 0.1 μM 3,3',5-triiodo-L-thyronine, 33 μM biotin, 10 μg/ml human transferrin and 1 μM dexamethasone). For the first 5 days, 250 μM 3-isobutyl-1-methylxanthine and 4 μM troglitazone were added to the adipogenic medium. For quantitative measurements of intracellular lipids, SVCs were grown to confluence and differentiated in type I collagen-coated 96-well plates for 16 days, then assayed using the AdipoRed adipogenesis assay reagent (Lonza) and a CytoFluor Multi-well Plate Reader series 4000 (PerSeptive Biosystems), according to manufacturers' instructions.

RNA isolation and qRT-PCR: Total RNA was extracted from WAT samples using TRIzol® reagent (Invitrogen), and from isolated mature adipocytes and cultured SVCs using the RNeasy Mini Kit (Qiagen). Between 0.5 and 1 μg of total RNA from WAT samples and SVCs, and 20-200ng total RNA from mature adipocytes, were reverse-transcribed into cDNA using the High Capacity cDNA Reverse Transcription kit (Applied Biosystems). Quantitative PCR assays were performed as previously described (Neville et al., 2011). Expression values were calculated by the ΔCT transformation method ($\Delta CT = \text{efficiency}^{[\text{calibrator Ct} - \text{sample Ct}]}$) and normalized to *PGK1* and *PPIA* in the case of tissue samples (Neville et al., 2011), and to *18S* in the case of mature adipocytes and SVCs.

Western Immunoblotting: Whole cell lysates were prepared in ice-cold lysis buffer containing 50 mM Tris pH8.0, 250 mM NaCl, 5 mM EDTA, 0.5% Igepal CA-630, 10 mM sodium fluoride, 1 mM sodium orthovanadate and protease inhibitors (Complete EDTA-free, Roche). Equal amounts of protein were resolved by SDS-PAGE, transferred onto polyvinylidene fluoride membrane (Biorad) and immunoblotted with the following antibodies according to the manufacturer's instructions: anti-LRP5 (D80F2) rabbit mAb (#5731; Cell Signalling), anti-phospho-LRP5/6 (Ser1490) rabbit pAb (#2568; Cell Signalling), anti-active

β-catenin (8E7) mouse mAb (05-665; Merck Millipore), anti-phospho-JNK (Thr183/Tyr185) rabbit pAb (#9251; Cell Signalling), anti-total JNK mouse mAb (sc-7345; Santa Cruz Biotechnology), anti-phospho-CaMKIIα (Thr286) rabbit pAb (sc12886-R; Santa Cruz Biotechnology), anti-total CaMKII rabbit pAb (sc-9035; Santa Cruz Biotechnology), anti-phospho-AKT (Ser473) rabbit pAb (#9271; Cell Signalling), anti-phospho-Erk1/2 (Thr202/Tyr204) rabbit pAb (#9101; Cell Signalling), anti-phospo-IRS1 (Tyr612) rabbit pAb (#09-432; Millipore), anti-α-tubulin rabbit pAb (ab15246; Abcam) and HRP-conjugated goat anti-actin pAb (sc-1616; Santa Cruz Biotechnology); followed by the appropriate horseradish peroxidise-conjugated secondary antibodies (DAKO) and detection by enhanced chemiluminescence (GE Healthcare). Densitometric analysis was performed using ImageJ (NIH, USA).

Measurement of adipocyte size and number: Adipocyte cell size measurements were performed as follows: Briefly, 5-µm sections of paraffin-embedded WAT biopsies were cut, dewaxed and stained with hematoxylin-eosin. Sections were photographed under 10x magnification and adipocyte cross-sectional area was determined using Adobe Photoshop CS2 9.0.2 (Adobe Systems, San Jose, CA) and the Reindeer image processing toolkit (Reindeer Games, Gainesville FL).

Mean adipocyte volume and weight were calculated for each individual using the following formulae:

$$V = \frac{\sum_{i=1}^{n} \left(\frac{\pi \times d^3}{6}\right)}{n}, \; w = V \times 0.915$$

V = mean cell volume (µm^3), d (real cell diameter) = histological cell diameter (µm) $\times$ 1.1 (Ashwell et al., 1976), w = mean weight of a single adipocyte (µg), n = total adipocyte number, density of fat cell triglycerides = 0.915 g/ml. Adipocytes were assumed to be

spheres. Abdominal adipocyte number was estimated by dividing DXA-derived android fat mass by mean adipocyte weight.

Supplemental References

Ashwell, M., Priest, P., Bondoux, M., Sowter, C., and McPherson, C.K. (1976). Human fat cell sizing--a quick, simple method. J Lipid Res *17*, 190-192.

Duncan, E.L., Gregson, C.L., Addison, K., Brugmans, M., Pointon, J.J., Appleton, L.H., Tobias, J.H., and Brown, M.A. (2009). Mutations in LRP5 and SOST are a rare cause of high bone mass in the general population. Bone *44*, S340-S341.

Gregson, C.L., Paggiosi, M.A., Crabtree, N., Steel, S.A., McCloskey, E., Duncan, E.L., Fan, B., Shepherd, J.A., Fraser, W.D., Smith, G.D., et al. (2013). Analysis of body composition in individuals with high bone mass reveals a marked increase in fat mass in women but not men. J Clin Endocrinol Metab *98*, 818-828.

Neville, M.J., Collins, J.M., Gloyn, A.L., McCarthy, M.I., and Karpe, F. (2011). Comprehensive human adipose tissue mRNA and microRNA endogenous control selection for quantitative real-time-PCR normalization. Obesity (Silver Spring) *19*, 888-892.

Vasan, S.K., Neville, M.J., Antonisamy, B., Samuel, P., Fall, C.H., Geethanjali, F.S., Thomas, N., Raghupathy, P., Brismar, K., and Karpe, F. (2011). Absence of birth-weight lowering effect of ADCY5 and near CCNL, but association of impaired glucose-insulin homeostasis with ADCY5 in Asian Indians. PLoS One *6*, e21331.